THE AMERICAN MINERALOGIST
JOURNAL OF THE MINERALOGICAL SOCIETY OF AMERICA

Vol. 27 JANUARY, 1942 No. 1

VARIATION IN THE PROPERTIES OF PYRITE[1]

F. GORDON SMITH, *University of Toronto, Toronto, Canada.*

ABSTRACT

Thirty-seven crystals of pyrite representing a wide range of habit, locality, and mode of occurrence, vary as follows: composition, $FeS_{1.94}$ to $FeS_{2.01}$ (10 analyses); specific gravity, 5.000 to 5.025 (10 crystals); optical anisotropism, none to strong; specific resistance at 20° C., in known and random directions, 0.014 to 256 ohms/cm. cube; temperature coefficient of resistance, −214 through zero to +26.5; thermo-electric potential against copper, strongly negative, through zero, to strongly positive, and often different in different parts of one crystal. Well developed lineage structure, with the "trunk" following a body-diagonal of the cube, is shown by one crystal.

These variations are explained mainly in terms of two variables: sulphur deficiency, giving Fe-atoms in S-positions and increasing the metallic character and conductivity; lineage structure giving interruptions of the crystal structure and reducing the conductivity. There is an indication that optically anisotropic pyrite is formed below 135° C. by regular arrangement of Fe-atoms in S-positions.

INTRODUCTION

Pyrite is generally regarded as a mineral with unusually constant properties. One property, namely the electrical conductivity, is known, however, to differ greatly in different specimens. In a recent study (1940) this variation was confirmed but no satisfactory explanation was found. The present work represents a continuation of the previous study, using the same material as before and the same specimen numbers, together with some further crystals. To the observations previously recorded, further data on the specific electrical resistance are added, together with observations on the following properties which were previously not treated or only briefly mentioned: temperature coefficient of resistance; thermo-electric potential; composition; density; optical behaviour and heat-treatment in relation to atomic structure; secondary crystal structure; crystal habit, colour and lustre. The new observations illuminate the previously unsolved problem and suggest an explanation of the surprising variation in conductivity.

Pyrite was studied in this manner for two reasons: it is a typical ex-

[1] This work was carried out with the aid of a scholarship of the National Research Council of Canada; published with the permission of the Council.

ample of a crystalline compound with properties between metallic and homopolar; and since most of the ore minerals lie between these limits, many of the types of variation found in pyrite might be expected in the other ore minerals. Furthermore, since pyrite is so frequently found in ore deposits, the variation of its properties, combined with geological evidence, might lead to criteria for recognizing the conditions of deposition of the associated ores.

The author wishes to thank Professor M. A. Peacock for extensive assistance with many phases of this work. Thanks are also due to Professor L. Gilchrist for the loan of electrical equipment, to Professor H. G. Smith for criticism of the manuscript, to Dr. A. A. Brant for help with the electrical theory, to Professor L. J. Rogers for chemical analyses, to Professor F. E. Beamish for spectroscopic analyses, and to Professor E. S. Moore for laboratory facilities.

Electrical Resistance at Constant Temperature

In the previous work (1940) the specific resistance (ρ ohms/cm. cube) was measured at room temperature on numerous right prisms cut in oriented and random directions from crystals of pyrite, using mercury electrodes. From prisms cut in various directions from one crystal it was found that the specific resistance along a unique body-diagonal of the cube was 20 times as great as the specific resistance along a direction at right angles to the unique direction. In different crystals the ratio of the greatest to least resistivity was about 10,000 to 1.

In the present work it was found that the resistance of some crystals of pyrite changes rapidly with temperature. It was therefore necessary to make a new set of measurements at constant temperature. This was done in the previously described manner, the temperature being held at $20 \pm 1°$ C. by enclosing the prisms in a tube in a water-bath.

One new crystal of pyrite was studied, namely No. 37, from Elba. It was a small pyritohedron, with fine striations perpendicular to the cube edges. The prism for electrical measurements was cut so that the edges were parallel to the crystallographic axes.

The new results for the specific resistance ($\rho_{20°}$) are given with the crystallographic direction of measurement in Table 3. As might be expected, the new values are similar to the old ones, but not exactly the same.

Temperature Coefficient of Resistance

The temperature coefficient of resistance of a substance at $t°$ C. is defined as the rate of change of specific resistance with temperature, divided by the specific resistance at 0° C., or

$$\alpha_t = \frac{1}{\rho_0} \cdot \frac{d\rho}{dt} \quad \ldots\ldots\ldots\ldots\ldots\ldots\ldots\ldots\ldots\ldots (1)$$

As is well known, the coefficient is positive for metallic substances; but it has often been reported negative for semi-metallic substances. Cases are known, for example, graphite, where the sign changes from negative at very low temperatures to positive at room temperature (Giauque, 1936).

Dean and Koster (1935) proved the variability of the sign of the temperature coefficient in the semi-metallic compound galena (PbS), and showed that there is a direct connection between the size of the solid aggregates making up the conductor and the sign of the coefficient. With small particle sizes the resistance was high and the coefficient was large and negative; but when the conductor was made up of a single crystal the resistance was smaller and the coefficient was small and positive. The theory put forward to explain this relation was that a compact single crystal of galena has a positive temperature coefficient similar to the metals; but if lattice discontinuities exist, some of the conducting electrons are bound at the interfaces, but can be released by thermal agitation. This effect of electron binding at lattice breaks has a greater effect on semi-conductors than on good conductors, as a larger percentage of the total number of conducting electrons is thus affected.

The temperature coefficient of resistance of pyrite has been reported to be positive for some crystals and negative for others (Mellor, 1935, pp. 215–216). Beckman (1912) found that the resistance increased with temperature as for metals, but that the relation between resistance and temperature was more accurately expressed by a formula:

$$\rho = \rho_0 e^{\alpha T}$$

where T is the absolute temperature. Koenigsberger and Reichenheim (1906) showed that the curve relating resistance and temperature reaches a minimum in the vicinity of 0° C. Since there is good evidence that the temperature coefficient of resistance is different in different specimens of pyrite, this coefficient was determined for most of the pyrite crystals used for resistance measurements.

From preliminary measurements it was found that the resistance of some of the pyrite crystals increased, and of others decreased, on heating. Prism 22, with the greatest specific resistance, was found to have a very large negative coefficient, and the complete relation between resistivity and temperature was found between 0° and 200° C.

The electrical contacts were of copper, electroplated to two opposite ends of the prism, with flexible copper cables soldered to the copper contacts. The prism was dried over phosphorus pentoxide for 7 days, quickly

dipped in varnish, and after this was dry, thickly coated with cellulose nitrate. A mercury thermometer and the pyrite prism were then sealed together in a small cement casing and immersed in a water bath for temperatures from 0° to 50° C. and in an oil bath from 50° to 200° C. The resistance at the various temperatures was found as before with a Megger resistance tester.

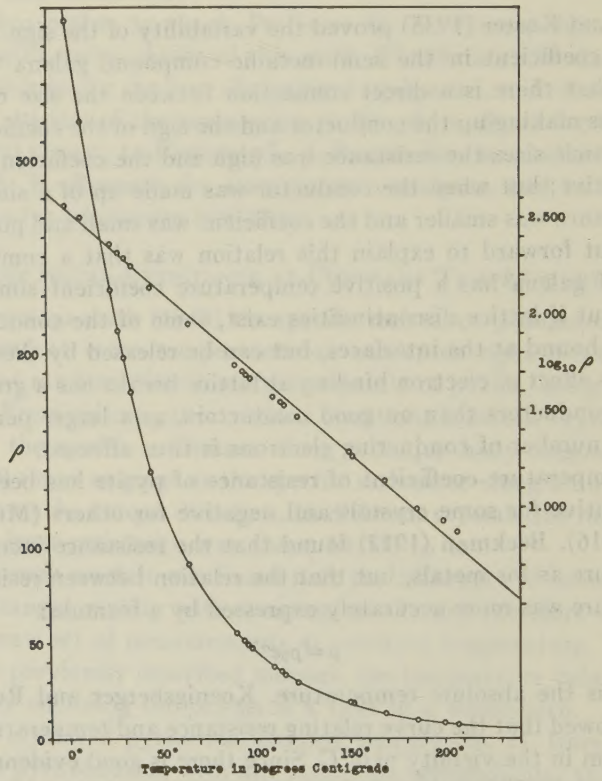

FIG. 1. Observed relation of specific resistance and logarithm of the specific resistance to temperature on pyrite crystal No. 22, with the largest negative temperature coefficient of resistance.

The data are shown in Fig. 1, with the specific resistance and the common logarithm of the specific resistance plotted against the temperature in degrees Centigrade. The relation is very nearly exponential, the equation for the entire 200° range being:

$$\rho = 71600e^{-0.0195T}$$

where ρ is the specific resistance and T is the temperature in °K.

The equation relating resistivity and temperature for the above crystal is of the form:

$$\rho = k \cdot e^{-\alpha T} \quad \ldots\ldots\ldots\ldots\ldots\ldots\ldots\ldots (2)$$

Assuming that this type of equation holds good for the other crystals, the value of the constant α was found directly from the values of ρ at two temperatures using the relation:

$$\frac{\Delta \log \rho}{\Delta T} = -\alpha \quad \ldots\ldots\ldots\ldots\ldots\ldots\ldots\ldots (3)$$

The coefficient of resistance as usually defined, equation (1), does not remain constant over a large range of temperature for these crystals. However, the constant α in equation (2) can be written:

$$-\alpha = \frac{1}{\rho} \cdot \frac{d\rho}{dt}$$

Therefore, at temperatures near 0° C., it is approximately equal to the ordinary coefficient, which can be treated as constant over any small range.

The specific resistance of each of the prisms of pyrite was found at 20° as described before, and at 100° when the tube containing the prism and its mercury contacts was suspended in a current of steam. The approximate temperature coefficient of resistance α, calculated as above, is shown in Table 3. The coefficient for the majority of the specimens was negative, for a few it was sensibly zero, and for the rest it was positive. It was also different in the three directions of measurement in most of the prisms.

Using the best data in the *International Critical Tables*, α and $\rho_{20°}$ were calculated for gold, silver, copper, lead, antimony, and bismuth, the results being as follows:

	Ag	Au	Cu	Pb	Sb	Bi
$\alpha \times 10^4$	35	25	38	30	34	32
$\rho_{20°} \times 10^6$	1.65	2.44	1.69	22	41.7	128

It was assumed that these measurements were made on compact, ideal crystals. It will be noted that the coefficient is always positive, and about 1/273 for all the metals.

The early investigations suggested that there might be a relation between the coefficient α and the specific resistance. On plotting α against $\log_{10} \rho_{20°}$ it was found that smooth curves could be drawn through the

points representing the three directions of measurement on single prisms, and that these slope in the same general direction (Fig. 2). The higher the resistance, the more negative the coefficient. This is also apparent from the general distribution of all the points.

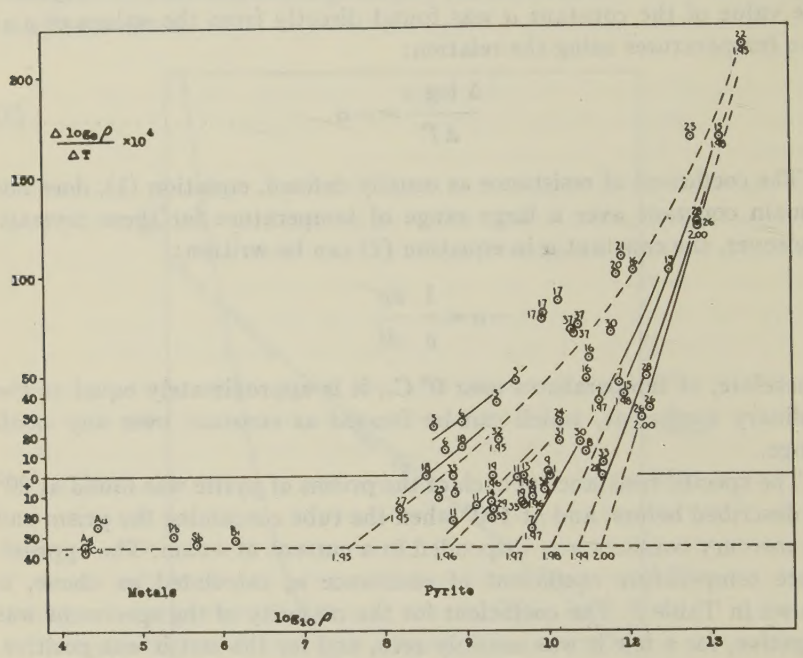

FIG. 2. Family of curves relating the approximate temperature coefficient of resistance to the logarithm of the specific resistance of specimens of pyrite numbered as in Table 3.

The equivalent points for Ag, Au, Cu, Pb, Sb, and Bi were also plotted, and it will be seen that these points lie very nearly on the straight line representing the constant value $\alpha = 1/273$. Some of the points for pyrite tend to approach this line, suggesting that the samples in question approach metallic behaviour.

According to the theory outlined above, these results are to be expected. A crystal with a high resistance and large negative thermal coefficient of resistance is one containing a large number of lattice discontinuities. The imperfections have some degree of regularity of position, since both the resistivity and the coefficient are different in different directions in most of the crystals of pyrite. The type of crystal imperfections and the reason for all the points in Fig. 2 not lying on one curve will be discussed later.

Thermo-Electric Potential

When an electrical circuit contains two different conductors and one of the contacts between them is warmed, a current is set up in the circuit. The potential developed is dependent on the character of the two conductors and the difference in temperature at the cold and hot junctions. The sign convention is that a conductor *A* has a positive thermo-electric potential to another conductor *B*, if the resulting current flows from *B* to *A* at the hot junction.

The thermo-electric potential of pyrite has been reported to be positive, negative and both positive and negative on the same crystal (Mellor, 1935, p. 216). Rose (1870) believed that the positive or negative potential was directly related to the positive or negative crystal forms. This was criticized by Friedel (1874), but Tutton (1911, p. 168) again stated that the sign of the hemihedral forms present determined the sign of the potential.

There seems to be no theoretical basis for relating the crystal habit and thermo-electric potential. However, the potential must be very closely connected with the temperature coefficient of resistance, since this determines whether the density of conducting electrons increases or decreases on heating.

The thermo-electric potential difference against copper was determined qualitatively for most of the pyrite crystals in the following manner: a clean copper wire was connected to the pyrite by pressure with the hand, and the end of a heated copper wire was touched to any equivalent place on the pyrite. The deflection of a millivoltmeter connected to the two copper wires was observed when contact was made. Preliminary work showed that all the specimens with a large negative temperature coefficient of resistance had a positive thermo-electric potential difference against copper, but for those with large resistivities, the amount of the deflection was small. This is due to the very large internal resistance of the specimen being studied, when compared with the resistance of the instrument.

The direction and amount of the deflection was noted when contact was made with crystal faces and saw-cuts through the centre of the crystals. The potentials corresponding to the instrument deflections are shown in Table 3. In some cases considerable zoning parallel to the faces was observed. In nearly every crystal showing zoning, the potential near and on crystal faces was more positive than in the centre of the crystal.

From an examination of the data, the relation between thermo-electric potential and thermal coefficient of resistance is established. Those crystals of pyrite with positive, zero, and small negative coefficients had

negative potentials against copper, and those with large negative coefficients had positive potentials.

If the interpretation of the cause of negative thermal coefficient of resistance is correct, and also its relation to the thermo-electric potential, then most crystals of pyrite have a greater degree of secondary crystal imperfection near the faces than in the central part. That is, the larger the crystal has grown, the more imperfect the lattice continuity. This will be discussed more fully later.

Composition

Many recorded analyses of pyrite show a deficiency in sulphur. A summary of a few newer representative analyses mostly from Doelter (1926, p. 527) is given in Table 1.

Table 1. Analyses of Pyrite

Spec. No.	1	2	3	4	5	6	7	8
Fe	47.10	46.84	47.00	46.49	46.20	46.66	47.28	46.51
S	52.97	51.97	52.50	53.49	52.81	53.06	52.89	53.26
Cu	—	tr.	—	—	—	—	—	—
SiO_2 or insol.	—	0.52	—	0.04	1.00	0.08	—	0.59
	100.07	99.33	99.50	100.02	100.01	99.80	100.17	100.36
Calc. to 100% Fe	47.07	47.40	47.24	46.50	46.66	46.79	47.25	46.62
S	52.93	52.60	52.76	53.50	53.34	53.21	52.75	53.38
FeS_n	1.96	1.93	1.95	2.00	1.99	1.98	1.95	1.99

1—Miniera di Casall, Prov. Grosseto (Doelter, No. 21). 2—Parana, Brazil (Doelter, No. 24). 3—Elba (Doelter, No. 39). 4—Elba (Doelter, No. 40). 5—Rio Tinto, Spain (Doelter, No. 41). 6—Elba (Juza and Biltz, 1932, p. 274). 7—U. S. A. (Juza and Biltz, *loc. cit.*). 8—Central City Mine, Gilpin Co., Col. (Doelter, No. 25).

Harvey (1928) suggested that departure from the ideal formula might account for differences in the electrical properties of the ore minerals. However, no definite relation between any of the properties of pyrite and its composition seems to have been established.

Several crystals of pyrite were analyzed by the author. Small chips were taken in each case from the same part of the crystal from which the prism for electrical measurements was taken. The chips were ground in an agate mortar under alcohol and about 0.2 gm. was digested in a cold mixture of nitric acid, bromine and potassium bromide, followed by gentle heating. After removing silica by filtration, the iron was reprecipitated as hydroxide, filtered and ignited to oxide. The sulphur was precipitated as barium sulphate in a large volume of solution, filtered and

ignited. The ratio of sulphur to iron alone was determined, although most of the specimens contained silica which was not weighed. The results, quoted as the atomic ratio in FeS_n, are shown in Table 3.

Professor L. J. Rogers kindly analyzed several crystals of pyrite for iron and sulphur. Iron and sulphur were determined on separate portions of the pulverized material, the former by titration and the latter by precipitation as barium sulphate after fusion in a bomb with sodium carbonate and peroxide. The results are given in Table 2.

TABLE 2. ANALYSES OF PYRITE

Spec. No.	32	7	13	15	19	26
Fe	45.5	46.35	45.85	45.95	45.80	45.9
S	51.0	52.25	51.5	52.2	51.5	53.1
	96.5	98.60	97.35	98.15	97.30	99.0
Calc. to 100% Fe	47.2	47.0	47.1	46.8	47.1	46.3
S	52.8	53.0	52.9	53.2	52.9	53.7
FeS_n	1.95	1.97	1.96	1.98	1.96	2.01

The atomic ratio, FeS_n, is also shown in Table 3, the asterisk denoting the results of Professor Rogers' analyses.

The effect of impurities on the properties of pyrite is problematical. Head (1934) has postulated that the gold in auriferous pyrite occurs as sheets along lattice discontinuities, and if present, one would expect the gold to increase the conductivity. However, the best-conducting specimen, No. 27, was analyzed spectroscopically by Professor F. E. Beamish and he reported it very pure, with no gold, a minute trace of manganese ($<0.0001\%$) and no other metals above 0.0001%. Tests were made for arsenic on No. 26 and No. 27 by Professor Rogers with negative results. A colorimetric test of No. 26 for nickel, using dimethylglyoxime, was negative.

The analyses show that pyrite may vary from $FeS_{2.00}$ to $FeS_{1.94}$ and still contain essentially nothing but iron and sulphur. When the formulas for the analyzed crystals were added to the points in Fig. 2, it became clearer why all the points did not lie on one line. While not without exception it appears that the points lie on a family of curves, one for each composition interval, $FeS_{1.95}$, $FeS_{1.96}$, and so on. There are thus two variables controlling the electrical properties of pyrite. When the composition remains constant, the temperature coefficient becomes larger negative and the resistance increases as the number of lattice discontinuities increases. However, for any one degree of such secondary crystal

imperfection the resistance decreases as the crystal becomes more deficient in sulphur.

It must be kept in mind, however, that the series of curves in Fig. 2 are in the nature of a generalization, and no precision is claimed. The zoning observed in some crystals may be in part compositional,[2] and there was no real assurance that the electrical measurements were performed on material exactly the same as that analyzed.

Density

The recorded density of pyrite (Doelter, 1926, p. 547) shows a range of 5.2 to 4.6. Kenngott found in 10 selected crystals that the density varied from 5.000 to 5.028. Allen, Grenshaw and Johnston gave the density of pure pyrite as 5.02, and pyrite from Elba, 5.027. The density calculated from the cell dimensions given by Peacock and Smith (1941) is 5.003 for $FeS_{2.00}$ and 5.014 for $FeS_{1.98}$.

It was thought that density determinations on the pyrite crystals would show, independently of the electrical criteria, the degree of crystal imperfection. The difference between the calculated density ($G_{calc.}$) and the measured density ($G_{meas.}$) would thus be a means of calculating the amount of open space due to lattice discontinuities. Single crystal fragments had to be used, and the Berman density balance was found to be well suited for this purpose. The absolute density values were determined by comparison with a diamond crystal as described by Peacock and Smith (1941).

The density of fragments weighing 20 mg. was determined for several of the analyzed crystals of pyrite, using toluene as the immersion liquid. In most cases the average of at least three similar values was taken, more weight being placed on the density of those fragments with clean conchoidal bounding surfaces and less on those with rough surfaces. The results are shown as $G_{meas.}$ in Table 3, opposite the corresponding theoretical density $G_{calc.}$, interpolated from the results of Peacock and Smith (1941). The measured density tended to approach the theoretical density, but was considerably lower in some cases, notably for No. 22.

Let it be assumed that lattice discontinuities do occur in pyrite, and that they are filled by air ($G = 0.001$). Then the relation between $G_{calc.}$, $G_{meas.}$, and the percentage volume of the crystal occupied by air in lattice discontinuities, S, is as follows:

$$S = \frac{G_{calc.} - G_{meas.}}{G_{calc.} - 0.001} \times 100\%.$$

[2] In the case of No. 27 the analysis of the part of the crystal whose electrical properties were studied gave $FeS_{1.95}$ while analysis of two other parts gave $FeS_{1.99}$ and $FeS_{1.97}$

Using this relation, S was calculated and is shown in Table 3. It is also shown plotted against $\log_{10}\rho_{20°}$ in Fig. 3. When the composition of each specimen is indicated as shown, a series of curves can be drawn, one for each composition interval, and this figure then becomes similar to Fig. 2. The resemblance probably means that secondary crystal imperfection and thermal coefficient of resistance *are* closely related, as postu-

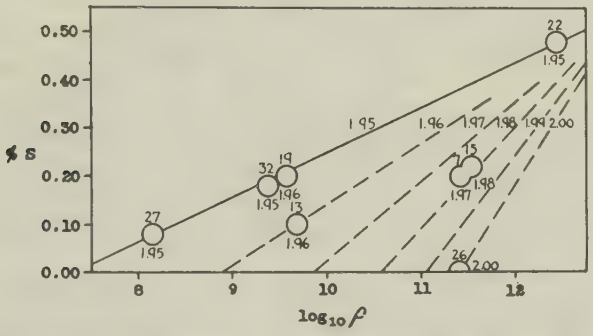

FIG. 3. Relation between percentage of open space and logarithm of the specific resistance of specimens of pyrite of known composition and specific gravity.

lated. For instance, prism 22 has the highest resistance, the most negative thermal coefficient of resistance and also the lowest density, all of which may be referred to a high degree of crystal imperfection. Direct evidence of the character of the crystal imperfection of this crystal will be described later.

Optical Behaviour and Crystal Structure

The crystal structure of pyrite is well known. It is cubic face-centered, and the relation of the iron and sulphur positions are such that if the iron atoms are at the lattice points, the sulphur atoms are in pairs whose axes are in the directions of the four non-intersecting body-diagonals. If one sulphur atom in a like position in every unit cell is replaced by iron, then the symmetry of the structure is changed from cubic to ditrigonal polar, and the formula becomes $FeS_{1.4}$. It has been shown by Peacock and Smith (1941) that iron may replace sulphur in pyrite. It is also generally known that pyrite is sometimes slightly anisotropic in polarized light. Smith (1940) has shown that the electrical resistance symmetry of one crystal of pyrite studied was rhombohedral (ditrigonal) and that heating to 135° C. rendered an optically anisotropic specimen isotropic.

An experiment was carried out to see if the symmetry of the optical anisotropism is the same as that of the electrical anisotropism. A cube

truncated by artificial octahedron planes was cut from a fragment of a cubic crystal from Leadville. All the faces were then polished by hand on a lap. On examination in polarized light, with the nicols very nearly crossed, all the cube faces were distinctly anisotropic. The position of the cube faces giving maximum blue and maximum red colors was such that the vibration directions of the nicols were parallel to face diagonals. Octahedron faces normal to the remaining body diagonal were isotropic. Thus the crystal is uniaxial and possibly ditrigonal.

Optical anisotropism of pyrite has been suggested by Schneiderhöhn (1930) to be due to the presence of arsenic. This cannot be the only explanation, since specimens Nos. 26 and 27, with no detectable arsenic, were moderately anisotropic. It is here postulated that when iron replaces some sulphur in pyrite, the replacement may take place in a random or regular manner. When random, the crystal remains isotropic, but when regular, it develops ditrigonal symmetry, with one of the cube body diagonals as the unique axis.

An attempt was made to determine the exact temperature at which anisotropic pyrite may become isotropic. A small plane parallel to a cube face on a large cubic crystal from Leadville was polished by hand on a lap. The section was distinctly anisotropic in reflected light. The polished face was protected by a coating of cellulose nitrate and the fragment was suspended in water and oil baths for 30 to 60 minutes at various temperatures between 100° and 214° C. The section was lightly polished after each heating and examined as before. No noticeable change in the degree of anisotropism was noticed during the series of heat treatments.

The effect of large crystal size on damping the transition was considered. A number of fragments of various sizes from an unheated part of the same crystal as the above were enclosed in a glass tube and heated in the oil bath to $214° \pm 0.5°$ C. for 15 minutes. They were then mixed with a hard wax and polished. One of the larger pieces, one about 3×2 mm. in section, was slightly anisotropic and all the rest were isotropic. It was evident that the smaller the size of the crystal fragment, the more readily the transition takes place.

Since only the moderate heating during mounting in bakelite is sufficient to destroy the anisotropism of some crystals of pyrite, a number of chips from most of the crystals of pyrite were mounted for polishing in a hard wax. The maximum temperature reached by the chips was about 70°C., and cooling to room temperature took about 10 seconds. A number of pieces were embedded in holes in a bakelite mould and were then polished by a Harvard-type machine.

On examination in plane-polarized light, about one-half of the fragments of pyrite were found to be anisotropic. The interference colors

with the nicols crossed, or nearly crossed, were shades of blue or blue-green and red or orange. With very weak anisotropism the colors were steel-grey to buff-grey. Four color changes were seen in every case during one complete rotation of the stage.

Only one set of randomly-oriented chips was examined; therefore the relative degree of anisotropism seen between different specimens could not be taken as the relative degree of anisotropism of the crystals from which they were taken. However, two degrees of anisotropism were recognized, relatively strong (*s*) and weak (*w*), as well as the isotropic (*o*) variety, and these are recorded in Table 3.

A few generalizations can be made from the above observations. Those crystals, thought to have been formed at high temperatures, such as cubes in schist and from pneumatolytic deposits (Nos. 4, 5, 18) were isotropic, and one known to have been formed at a low temperature, the Joplin pyrite (No. 23), was anisotropic. Many of the isotropic crystals were assumed to be sulphur-deficient, both from their place on the series of curves of Fig. 2 and from their density. Since they are isotropic, the iron replacing sulphur must be in purely random positions. It is reasoned that if an anisotropic crystal becomes isotropic on heating and does not return to its original condition on cooling, the originally somewhat ordered condition of the lattice irregularity (iron in sulphur positions) becomes irreversibly disordered or random. As both isotropic and anisotropic sulphur-deficient pyrite exists in nature, the former is postulated to have formed above and the latter below, some critical temperature, which is believed to be between room temperature and 135° C.

Secondary Crystal Structure

Various theories of secondary crystal structure have been postulated to explain the departure from the theoretical strengths and other properties of crystalline solids. The proof of regular secondary structure is not conclusive and Buerger (1934*b*) has vigorously contested the theory from which such structures were deduced. However, a secondary structure which is not regular but is a morphological phenomenon of crystals, has been described and has been given the name *lineage structure* by Buerger (1934*a*).

Buerger (1934*a*) considers the growth from a crystal nucleus to be branched, very much like a filled-in dendritic structure, the central part being called the trunk, the main subdivisions, branches, and the filling between them, boughs. The entire crystal is viewed as an agglomeration of units which when traced back from the crystal faces towards the nucleus, join with neighboring units. Imperfection of this sort may be non-existent, giving an ideally perfect crystal, or great, giving an ideally

imperfect crystal. It may be so well developed that the crystal aggregate becomes an arborescent group of radiating crystals rather than one crystal.

Among the pyrite crystals studied, a few were nearly perfect in the foregoing sense, showing plane, mirror-like faces; but most of them had faces that gave a wavy reflection. No. 22 was so imperfect that the cube faces were rounded and partly covered by neighboring cube and octahedron secondary terminations mutually inclined up to 20°. This suggested that lineage structure might correspond to the lattice discontinuities inferred to explain the electrical effects.

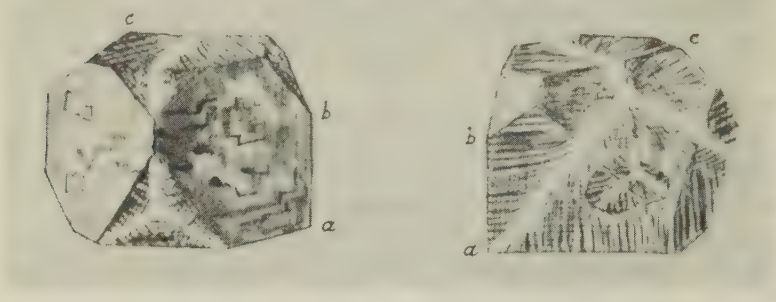

FIG. 4. Sketch of the lineage structure developed on pyrite crystal No. 22 after etching with concentrated nitric acid.

A cubical crystal, from a part of which prism No. 22 was obtained, was prepared for etching by grinding and smoothing the natural cube faces, and also grinding octahedron planes on the corners. The cube was then immersed in warm fuming nitric acid for about two minutes, washed and dried.

A very striking pattern had been etched into the surface. A sketch of the crystal, only slightly idealized, is shown in Fig. 4. One body diagonal of the crystal is a unique polar axis of three-fold symmetry. There are also three planes of symmetry intersecting in this axis. The symmetry may be considered to be ditrigonal polar. Following Buerger's terminology, one body diagonal is the trunk of the lineages. There are three main branches which divide the whole crystal into three zones, the boughs in each zone all growing parallel to each other and perpendicular to the three cube faces around one extremity of the trunk. In addition to the lineage structure, fine lines were seen running perpendicular to the boughs, parallel to the three cube faces mentioned above. The lines represent planes parallel to these cube faces, and possibly they are growth lines. While being prepared for density measurements, a fragment from

the same crystal showed a grain such that it broke much like a columnar basalt into shining rather irregular polygonal prisms approximately 1 mm. across. These were probably the main boughs in the filled-in part between the branches.

Several other crystals were etched on ground surfaces with nitric acid. The Joplin pyrite, No. 23, showed a well developed lineage structure, but in others only traces of this structure were evident. On those crystals inferred to be more nearly perfect from electrical measurements, either smooth surfaces were formed or small, regular, lenticular pitting.

From the interpretation of the electrical measurements, Nos. 22 and 23 were the two specimens with the greatest amount of lattice discontinuity. They also were the only two which had a lineage structure gross enough to be brought out by etching. This was thought to be sufficient evidence to state that the crystal imperfection in pyrite, detected by a negative temperature coefficient of resistance, is due to the development of lineage structure.

Earlier it was remarked that the positive thermo-electric potential increases outward from the centre of the crystals. This corresponds to an increase in crystal imperfection, here considered to be due to lineage structure.

Crystal Habit, Color and Lustre

In the older literature two kinds of pyrite were recognized, positive and negative. Positive pyrite was said to be characterized by striations on the pyritohedron parallel to the trace of the cube edge. That is, oscillatory combination between {021} and {001}. This variety was said to be a poor conductor of electricity and to have a positive thermo-electric potential against metals. The negative variety has striations on the pyritohedron perpendicular to the trace of the cube edge, formed by oscillatory combination of {012} and {124} or {112}. It is a good conductor and has a negative thermo-electric potential (Tutton, 1911, p. 168).

From the results of the previous work (1940) on 36 specimens of pyrite, it is apparent that there is no sharp division into good and poor conductors. Also from the tabulation of the thermo-electric potential on the same specimens, there is no basis for a sharp division. In fact some crystals are zoned gradationally from negative in the center to positive on the crystal faces. However, there must be some relation between these properties and the crystal habit, because the above relation has not been definitely disproved. Accordingly, the major crystal forms on most of the specimens were noted and are listed in Table 3, to see if any relations could be established with the other properties.

While not very definite, some generalizations can be made. The faces of any crystal showing the diploid had a negative thermo-electric poten-

tial to copper. Such crystals were good conductors, and from their position in Fig. 2, were also decidedly sulphur-deficient. However, No. 37, which showed the pyritohedron and diploid, so that the striations from their combination were perpendicular to the cube edges, was negative on the crystal faces, but positive in the interior of the crystal and had an average resistance. In addition, many crystals showing the pyritohedron and cube, which should from the older ideas be positive and poor conductors, were negative and good conductors.

The color and lustre of the pyrite crystals studied varied a little. The two crystals with the highest amount of sulphur, No. 15 ($FeS_{1.98}$ and No. 26 ($FeS_{2.00}$), were noticeably yellower and nearer a true brass color than those deficient in sulphur, which tended toward a rather pale brass color. The lustre of the former two was metallic, but also somewhat adamantine, and both were splendent. The sulphur-deficient varieties had a metallic lustre, from bright to somewhat dull.

The conclusion was reached that the composition plays some part in controlling the crystal habit, but the forms seen are indicative of only the outer part of the crystal. The interior may have different properties. The older concept of two distinct types of pyrite has not been confirmed. The only agreement is that a crystal with striations on the pyritohedron perpendicular to the trace of the cube edge is likely to be sulphur-deficient, a good conductor and thermo-electrically negative against copper, on the crystal faces and often in the interior as well. Pyritohedrons striated the other way, if the color is brassy and the lustre bright to splendent, are, at least on the surface, usually nearer the ideal composition, poor conductors and often thermo-electrically positive against copper.

Discussion and Conclusions

It is postulated that the variation of the properties of pyrite is a function of two independent variables. One is the composition and the other is the secondary crystal structure. The former is measured by departure from the ideal formula FeS_2, and this seems to be always in the one direction, toward a deficiency of sulphur. Iron takes the place of some sulphur in such crystals, and this is known to affect the lattice dimensions and probably also its symmetry. The secondary crystal structure observed is a growth phenomenon known as lineage structure.

Variation in composition seems to affect the conductivity of pyrite. Other things being equal, the lower the sulphur content of the pyrite, the lower the resistance. This is to be expected if iron replaces some sulphur in sulphur-deficient specimens. The unit of structure may be pictured as a pair of sulphur atoms each of which is in contact with three iron atoms. If an iron atom replaces one of the sulphur atoms, it is likely the bond type between the three iron atoms around the replacing iron

atom would be much more metallic than the iron-sulphur linkage.

The habit, color and lustre of pyrite also seem to be affected by variation in composition. A splendent metallic lustre and a brass color is characteristic of pyrite with nearly the ideal formula, while sulphur-deficient varieties have a bright to rather dull metallic lustre and a pale brass color. The crystals low in sulphur seem to favor the diploid more than those richer in sulphur.

It was inferred that iron replacing sulphur in sulphur-deficient pyrite may be in regular positions, giving optically anisotropic pyrite, or it may be in irregular positions, giving the isotropic variety. The regular replacement may be made random by heating above 135°C. and this change is irreversible over the short period of laboratory experiments. It is probably irreversible in nature, since isotropic pyrite with a deficiency of sulphur does occur. The hypothesis is presented that pyrite formed in nature above approximately 135°C. was isotropic and remained so when cooled to room temperature, but when formed below this temperature it was anisotropic. This provides another geological thermometer which should be of use in economic deposits. However, since the bakelite moulding temperature is above the order-disorder temperature, some other mounting medium should be used when the optical anisotropism of pyrite is being studied.

Secondary crystal structure has a very much greater effect than composition on the electrical properties. Crystals with a well developed lineage structure have a high resistance and a large negative temperature coefficient of resistance. There is some evidence that the reverse holds true: that nearly perfect crystals have a low resistance and a positive coefficient. The thermo-electric potential against metals is related very closely to the coefficient and so to the secondary structure. With the sign conventions as described above, those crystals with a positive, zero, or small negative coefficient have a negative thermo-electric potential against copper and those with a large negative coefficient have a positive potential.

The density of pyrite fragments is low when the crystal shows evidence of lineage structure. The difference between the density as measured and calculated is not great, however, which must mean that the interlineal spaces are very small.

The lineage symmetry on one crystal was found to be ditrigonal polar, a symmetry possible from a regular replacement of iron in sulphur positions. There is a tendency for those crystals with a relatively strong optical anisotropism (regular lattice replacement) to show a well-developed lineage structure, so that it is probable that a regular replacement with ditrigonal polar symmetry controlled the development of a lineage structure having the same symmetry.

TABLE 3. SUMMARY OF OBSERVATIONS ON PYRITE

No.	[uvw]	$\rho_{20}°$	$10+\log_{10}\rho_{20}°$	$\alpha\times10^4$	E Centre	E Face	n	G_{calc}	$G_{meas.}$	S	Opt.	Habit
1	—	1.1	10.041	0.0	±	..	..	..	..	..	..	..
2	[110]	0.069	8.839	− 8.8	−−	..	..	..	..	..	0	*a c*
3	[111]	0.15	....	....	−−	..	..	..	..	..	0	*a e*
4	[100]	0.17	....	....	−	..	..	..	..	..	0	*a e*
5	—	0.23	9.362	− 36.6	−−	−−	..	..	..	..	0	*e*
	—	0.40	9.602	− 47.7								
	—	0.039	8.591	− 24.6								
6	—	0.052	8.716	− 13.1	−−	±	..	..	5.020	..	..	*e*
	—	0.086	8.934	− 27.2								
7	—	0.59	9.770	+ 26.5	++	+	1.97*	5.015	5.005	0.20	0	*a e*
	—	7.4	10.869	− 46.1								
	—	4.1	10.613	− 37.6								
8	[100]	2.83	10.452	− 12.0	..	..	..	..	..	..	..	..
9	[100]	0.98	9.991	− 2.1	−−	−	..	..	..	..	..	*e a*
10	—	7.03	....	....	+	..	..	..	..	..	*w*	..
11	—	0.125	9.097	+ 14.3	−−	..	..	..	..	..	..	..
	—	0.404	9.606	+ 0.9								
	—	0.064	8.806	+ 22.1								
12	—	1.7	....	..	±	..	..	..	..	..	*w*	..
13	—	0.470	9.681	0.0	±	..	1.96*	5.020	5.015	0.10	0	..
14	[100]	0.19	9.279	+ 13.1	−−	−	..	..	..	..	..	*a e*
15	[110]	132	12.121	−168	⊕	⊕	1.98*	5.011	5.000	0.22	*w*	*a e*
	[110]	8.6	10.934	− 40.3								
	[001]	31.6	11.500	−102								
16	[100]	3.16	10.500	− 58.5	± to +	⊕	..	..	..	..	0	*a e*
	[010]	2.94	10.468	− 48.1								
	[001]	11.4	11.057	−102								
17	[100]	0.860	9.934	− 78.1	++	+	..	..	5.025	..	*s*	*a e*
	[010]	0.886	9.947	− 81.3								
	[001]	1.35	10.130	− 86.9								
18	[100]	0.085	8.929	− 14.1	−−	−	..	..	..	..	0	*a o*
	[010]	0.030	8.477	0.0								
19	[100]	0.456	9.659	+ 13.4	−−	++	1.96*	5.020	5.010	0.20	0	*a e*
	[010]	0.613	9.787	+ 10.4								
	[001]	0.20	9.301	0.0								
20	[100]	7.05	10.848	−100	++	⊕	..	..	..	..	*s*	*a o*
21	—	8.26	10.917	−109	+	+	..	..	..	..	*s*	*o*
22	[100]	256	12.408	−214	0	0	1.95	5.024	5.000	0.48	*s*	*a o*
23	—	60.8	11.784	−168	⊕	⊕	..	..	..	..	..	*o a*
24	[100]	1.39	10.143	− 26.7	++	++	1.94	..	..	..	0	*a e*
25	—	0.043	8.633	+ 11.1	±	++	..	..	..	..	0	*e a*
26	[001]	17.7	11.248	− 33.6	⊕	⊕	2.01*	5.003	5.005	0.00	*w*	*a e n o*
	[110]	14.1	11.149	− 28.4			2.00					
	[110]	72.4	11.860	−124								
27	—	0.014	8.146	+ 16.6	−−	−	1.95	5.024	5.020	0.08	*w*	*e t o a*
28	[111]	70.7	11.849	−126	⊕	⊕	..	..	5.005	..	*w*	*a e n o*
	[110]	16.2	11.209	− 49.3								
	[112]	4.46	10.649	0.0								
29	—	0.20	9.301	+ 16.8	±	−	..	..	5.010	..	0	*t o*
30	—	5.88	10.769	− 71.4	− to ++	+	..	..	..	..	*s*	*e a*
	—	2.43	10.386	− 17.0								
31	—	1.35	10.130	− 17.5	− to ++	+	..	..	..	..	..	*a e o*
32	[100]	0.231	9.367	− 18.0	−−	−	1.95*	5.024	5.015	0.18	0	*a*
33	—	4.58	10.661	− 6.2	±	±	..	..	..	..	*w*	..
	—	0.19	9.279	+ 21.2								
	—	0.48	9.681	− 14.3								
34	[100]	0.87	9.940	− 7.1	−	..	..	..	..	..	..	*a e*
35	[100]	0.064	8.806	0.0	−−	++	..	..	..	..	..	..
36	[100]	5.0	..	..	− to ++	+	..	..	..	..	*s*	*e a*
37	[100]	2.34	10.369	− 74.9	++	−	..	..	..	..	..	*e t a*
	[010]	1.92	10.283	− 72.8								
	[001]	2.08	10.318	− 70.5								

Explanation of Table 3. No., specimen number. [*uvw*], crystallographic direction in which resistance was measured. $\rho_{20}°$, specific resistance in ohms/cm. cube. α, temperature coefficient of resistance, $\Delta \log \rho/\Delta t$. *E*, thermo-electric potential against copper as indicated by voltmeter deflections: −−, strong negative; −, weak negative; ±, weak, positive or negative; ++, strong positive; +, weak positive; ⊕, positive near zero; 0, zero. *n*, sulphur-iron ratio in FeS_n. G_{calc}, density calculated from cell dimensions and composition. $G_{meas.}$, measured density. *S*, calculated percentage open space. Opt., optical anisotropism: *s*, strong; *w*, weak; 0, none. Habit, observed forms in order of importance: *a*(100), *e*(210), *o*(111), *t*(421), *n*(211).

References

Beckman, B., *Versl. Amsterdam Acad.*, **21,** 1281 (1912).
Buerger, M. J., *Zeits. Krist.*, **89,** 195 (1934 *a*).
———, *Zeits. Krist.*, **89,** 242 (1934 *b*).
Dean, R. S., and Koster, J., *U. S. Bur. Mines*, Rept. Invest., No. **3268** (1935).
Doelter, C., *Handb. Mineralchem.*, **4** (1) (1926).
Friedel, C., *Compt. Rend.*, **78,** 508 (1874).
Giauque, W. F., *Ind. Eng. Chem.*, **28,** 743 (1936).
Harvey, R. D., *Econ. Geol.*, **23,** 778 (1928).
Head, R. E., *U. S. Bur. Mines*, Rept. Invest., No. **3226,** 27 (1934).
Juza, R., and Biltz, W., *Zeits. anorg. Chem.*, **205,** 273 (1932).
Koenigsberger, J., and Reichenheim, O., *Phys. Zeits.*, **7,** 572 (1906).
Mellor, J. W., *Comprehensive Treatise on Inorganic and Theoretical Chemistry*, **14** (1935).
Peacock, M. A., and Smith, F. G., *Univ. Toronto Studies, Geol. Ser.*, in press (1941).
Rose, G., *Sitzber. Akad. Berlin*, **333** (1870).
Schneiderhöhn, H., *Chemie der Erde*, **5,** 385 (1930).
Smith, F. G., *Univ. Toronto Studies, Geol. Ser.*, **44,** 83 (1940).
Tutton, A. E. H., *Crystallography* (1911).

INVESTIGATION OF THE MINOR ELEMENTS IN DIAMOND

Frank G. Chesley,

Massachusetts Institute of Technology, Cambridge, Mass.

Contents

	Page
Abstract	20
Introduction	20
Description of diamonds	21
Method of preparing samples	26
Spectrographic apparatus and technique	27
Choice of spectrographic method	28
Results of spectrographic analysis	28
Ultra-violet spectroscopy of diamond	32
X-ray examination	33
Fluorescence	34
Neutron bombardment	35
Summary	35
Acknowledgments	36

Abstract

The methods and results of emission spectrographic analysis of thirty-three diamonds are described. Thirty elements were analyzed for and thirteen were detected among the thirty-three diamonds. The elements Al, Si, and Ca form a persistent group which appeared as minor elements in every specimen. The elements Al and Si exhibited 'sympathetic' variation in each diamond. Absorption spectra in the ultra-violet region revealed the presence of a type 2 diamond which was found to be the purest of the thirty-three diamonds. Diamonds from some of the geographical localities show similarities in minor element content. The elements Fe and Ti tended to be present in the colored diamonds. A minor correlation was made between the crystal habit and the simultaneous presence of Ag and Ti. No correlation was observed between minor element content and fluorescence phenomenon.

Introduction

The primary objective of this investigation was to carry out a semi-quantitative analysis, based on emission spectra, of the impurities present in certain diamonds. An attempt has been made to correlate the information so obtained with the color, crystal habit, fluorescence, *x*-ray pattern, and geographical location of the diamonds. The results are also discussed on the basis of the two established types of diamonds.[1]

At the suggestion of Amos J. Shaler, J. K. Smit and Sons, Inc., kindly placed certain diamonds at the disposal of the writer for research purposes. It was decided to cleave the diamonds, using one half for emission spectra work, and to retain the other half for non-destructive observational purposes.

[1] Robertson, R., Fox, J. J., and Martin, A. E., Two types of diamond: *Phil. Trans. Roy. Soc.* (London), **A 232,** 463 (1933).

There are very few references[2,3] in the literature to the impurities which occur in the diamond. These references are incomprehensive in scope. This lack of information might be due to the difficulty in obtaining good specimens for research purposes, especially when they are to be partially destroyed to secure certain data.

The diamonds used in this investigation are considered to be quite a representative group, as they range from colorless to colored, and from those perfect in form to those quite imperfect.

Description of Diamonds

In the original lot of diamonds submitted for this investigation there were 138 stones from 15 different localities. The quantities and localities are tabulated in Table 1. From this quantity the writer was privileged to

Table 1

Name	No. of Stones in Original Lot	Weight in Carats*	No. of Stones Selected for Analysis
Angola	10	2.90	4
So. W. African Alluvial	5	1.13	2
Dark Brown Premiers	10	1.55	2
Congo Octahedrons	10	3.21	2
Sierra Leone	10	3.48	3
Brown Congo	10	2.75	2
Premier Black Ballas	10	2.95	1
Brazilian (Venezuela)	13	1.16	4
Brazilian Ballas	5	0.70	2
Kimberley	5	1.85	2
Carbonados (Brazil)	10	1.65	3
Brazilian (Bahia)	10	1.77	2
Congo Cube	10	2.83	2
French Guinea	10	2.55	2
West Africans	10	1.80	—
Total	138	32.28	33

* 1 carat = 0.200 gm. Av. wt. per stone = 0.235 ct.

select an average of two stones from each locality for use in the investigation. Particular care was taken by the staff of J. K. Smit and Sons, Inc., to assure validity of the sources of the diamonds. All of the diamonds are

[2] Among them the writer found:

Wild, G. O., and Klemm, R., Mitteilungen über Untersuchungen an Mineralien: *Centr. Mineral.*, **Abt. A.** 321 (1925).

[3] Walter, B., Eine characteristische Absorptionserscheinung des Diamanten: *Ann. Physik.*, **42,** 505 (1891).

from famous diamond producing regions in South America and Africa. The approximate geographic locations are shown in Fig. 1.

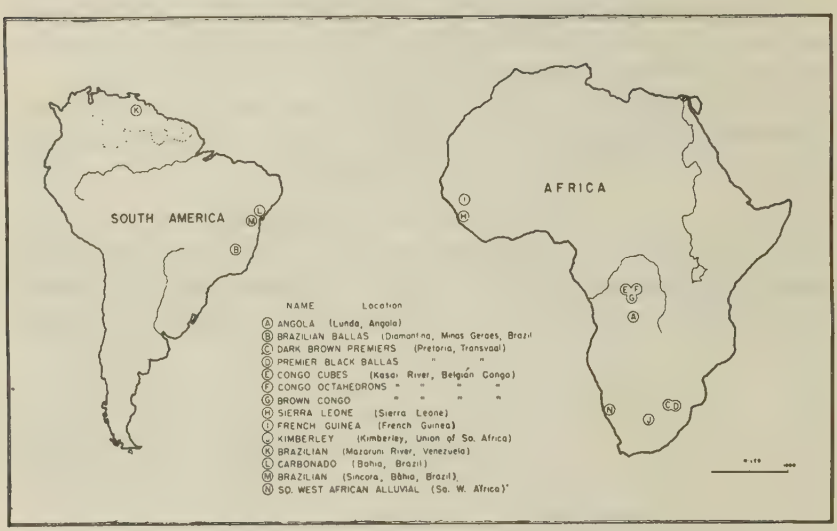

FIG. 1. Map showing approximate geographic locations of diamonds used in this investigation.

The choice of the representative stones from each locality was made with the intent to select individual stones that possessed dominant characteristics of certain types such as color, perfection of form, obvious lineage structure,[4] etc. The purpose of this choice was to see if any correlation could be found between these features and the data obtained from the emission spectra.

The colors of all the diamonds described below will be found in Table 2.

From Figs. 2 and 3 it will be seen that the various morphological features common to the diamond are well represented in the group. Nos. 1–4 are all highly twinned and were selected mainly on the basis of their imperfection of form and obvious evidence of lineage structure. Lineage structure is a common, though rarely mentioned, characteristic of diamond crystals. Attention was focused on this feature because of the importance it seems to have played in the extensive work carried out by Robertson, Fox, and Martin.[5] Diamonds 5 and 6 were selected on the

[4] Buerger, M. J., Lineage structure of crystals: *Zeits. Krist.*, **89**, 195 (1934).

[5] Robertson, Fox, and Martin have established the existence of two types of diamond as based on the positions of absorption bands in the infra-red and ultra-violet regions of the spectrum. They found the common, or type 1 diamond, to have an absorption band at 8μ in the infra-red region and complete absorption at 3000 Å in the ultra-violet. The rarer,

basis of perfection as fine octahedra. Likewise 9 and 10 were chosen as representatives of the octahedral habit, though from a different locality. Specimens 7 and 8 were interesting in so far as they were single crystals, colored, transparent, and apparently free from inclusions. The Sierra Leone diamonds, Nos. 11, 12, and 13, constitute a group from a single locale in which various habits and colors were represented. The brown Congos, Nos. 14 and 15, exhibited cleavages which showed excellent lineages, quite similar to those seen on galena cleavages. These stones were also colored. Number 16 was a grayish translucent diamond highly twinned with many steps present on the surface. Diamonds Nos. 17–20 were transparent, colored specimens. Numbers 21 and 22 were nearly spherical in shape and possessed much pitting or etching on the surface. The Kimberley stones, Nos. 23 and 24, were colorless. Both specimens exhibited very few natural faces, these few, however, indicated a dodecahedral habit. The carbonados, Nos. 25, 26, and 27, were selected because they were totally opaque and lacked any visual evidence of crystallinity. Diamonds Nos. 28 and 29 were clear transparent specimens each slightly colored. Both were distorted crystals, No. 28 being a distorted dodecahedron and No. 29 a distorted octahedron. Numbers 30 and 31 were chosen because of their color and cubic habit. Number 31 was a penetration twin. The French Guinea diamonds, Nos. 32 and 33, were cleavage fragments with only a few natural faces. No particular habit could be assigned to these specimens. Both appeared to have a slight pinkish tint.

A. F. Williams[6] has been in a unique position to observe many hundred thousand carats of diamonds. Referring to the color of diamonds he says:[7]

"The color of diamond is generally referred to as white or colorless, but as a matter of fact, this is one of the rarest colors found among diamonds . . . ."

---

or type 2 diamonds, have no band at 8μ and exhibit complete absorption at 2250 Å. They observed that a crystalline condition which was indicated by fine oscillation lamillae was more particularly associated with type 2 diamonds. The writers also state that 2 was more nearly isotropic optically than type 1, but specific gravity, index of refraction, dielectric constant, Raman effect, and fluorescence phenomenon showed no difference between the two types.

Another feature which they found common to the type 2 diamonds was a marked photoelectric effect. This same effect they observed to be very feeble in the type 1 diamonds. Robertson, Fox and Martin offer an explanation of the difference in transparency of the two types as derived from a consideration of the various modes of vibration of C against C in the diamond structure. They advance arguments against the assumption that the type 2 owes its properties to common impurities.

[6] Williams, A. F., The Genesis of the Diamond, Ernest Benn, Ltd. (London), p. 475 (1932).

[7] *Ibid.*, p. 467.

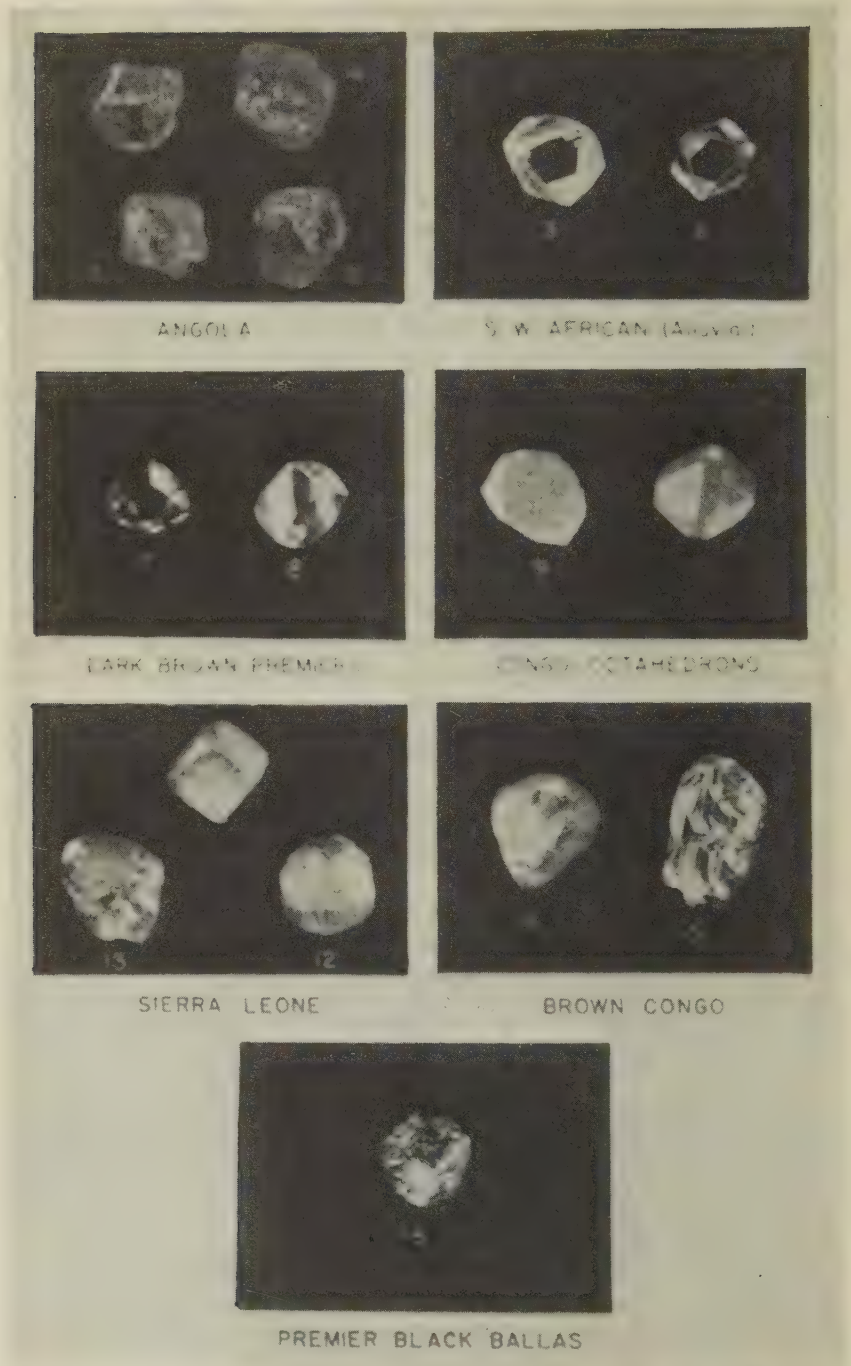

FIG. 2. Photographs of diamonds. × 4.

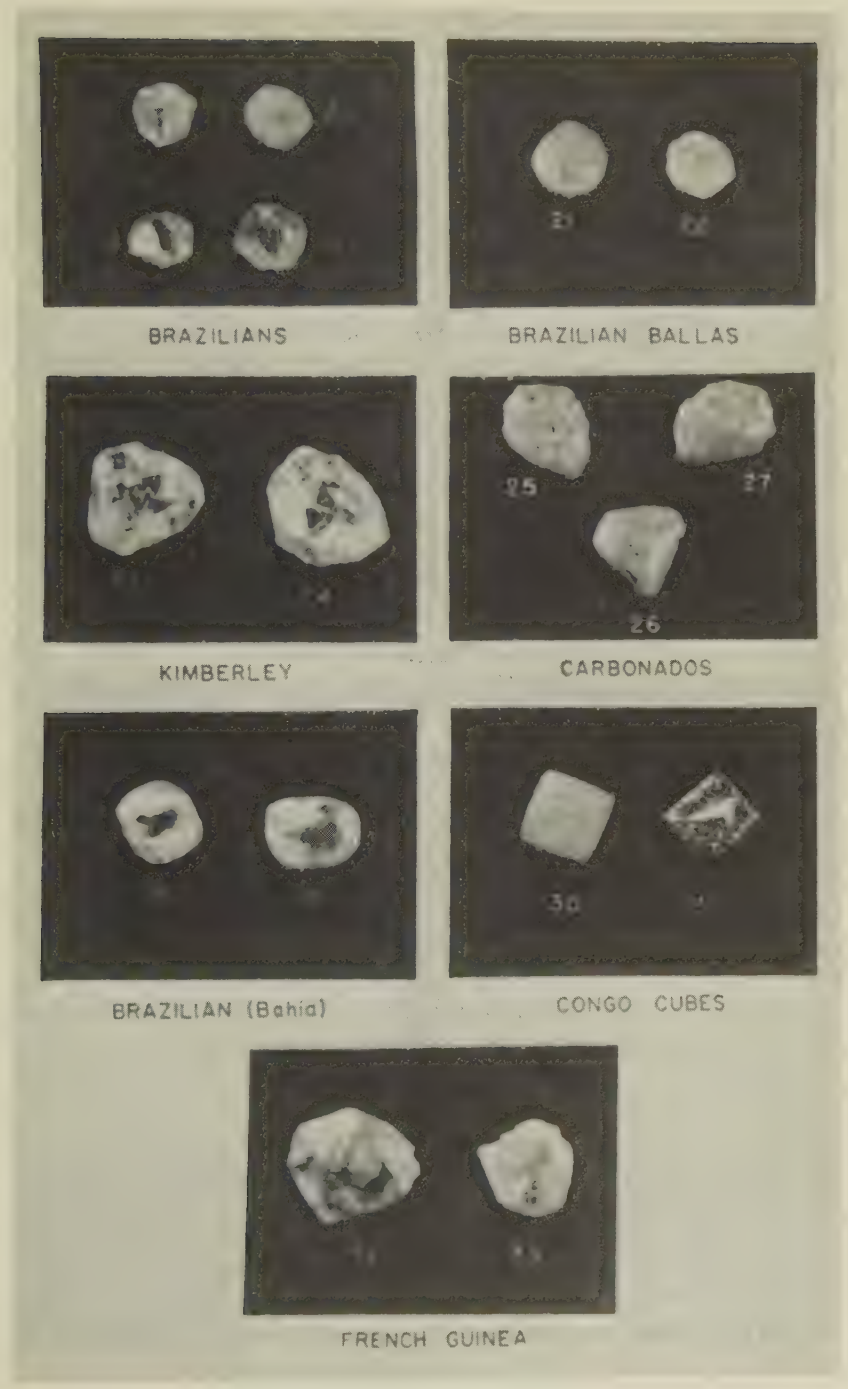

FIG. 3. Photographs of diamonds. × 4.

TABLE 2

Diamond No.	Color	Diamond No.	Color
1	colorless	18	very pale green
2	colorless	19	pale yellow
3	white	20	pale yellow
4	colorless	21	pale yellow
5	pale yellow tint	22	white
6	very slight yellow tint	23	colorless
7	brown tint	24	colorless
8	light brown tint	25	dark brown
9	clear colorless	26	black
10	grayish	27	black
11	dark green opaque	28	very pinkish tint
12	deep green	29	very pale green tint
13	dark green	30	yellow
14	brown	31	dark yellow green
15	slight yellow tint	32	light pinkish tint
16	dark gray transparent	33	light pinkish tint
17	clear very pale yellow		

METHOD OF PREPARING SAMPLES

Each of the diamonds selected weighed approximately 50 mg. Only a fraction of each stone was necessary for the spectrum analysis. Consequently every diamond was photographed for record purposes and then cleaved in half. One half of each stone was powdered for spectrographic examination because a single fragment would not stay in the arc long enough for satisfactory excitation. The powdering process consisted in shattering each stone by percussion. Although diamond is the hardest known mineral, a sharp blow will cause it to break into many small pieces. Each cleavage fragment was placed in an improvised mortar which was constructed as follows. Two cold-rolled steel slugs, which were $1\frac{1}{4}''$ diam. and $3/32''$ thick, held the diamond between them. The slugs were then placed on a short steel cylinder of slightly smaller diameter. A steel envelope was slipped over this assembly and another cylinder was inserted at the top. A few sharp blows on the top member reduced the diamond to powder. The envelope prevented the powder from shooting out laterally. The powder was then carefully gathered and cleaned. Two new slugs were used for each specimen.

Before the crushing process both the steel slugs and the fragment had been thoroughly treated with organic solvents to remove any grease or oils that may have been on them due to handling. After the crushing process the powder was placed under a magnet to remove any loose iron.

The powder was then subjected to vigorous acid treatment in order to remove any impurities that might have accumulated on the surfaces of the shattered particles. After moderate warming, the acid solution was diluted and decanted. This was followed by washing with distilled water, alcohol, and ether. All of the wet processes were carried out in small glass vials.

Spectrographic Apparatus and Technique

The apparatus used for this investigation was the 21 foot, 30,000 lines per inch, Wadsworth grating spectrograph of the Cabot Spectrographic Laboratory at the Massachusetts Institute of Technology. The region of the spectrum examined ranged from 2800 to 4600 Å. This range was selected because it includes the major portion of the sensitive lines of the elements which preliminary examination showed to be present in the diamond. The dispersion of the spectrograph in this region is 2.46 Å per millimeter. The spectra were registered on Eastman commercial film and developed for 6 minutes at 18 -20°C. in D-11 developer, diluted 1:1.

A 220 volt D.C. source with resistance and inductance in series was used for excitation purposes. The 220 volt supply gave a steady discharge and resistances were arranged in stages which permitted current increases from $3\frac{1}{2}$ to $7\frac{1}{2}$ to 12 amps. Each sample was ignited at a current of $3\frac{1}{2}$ amps and electrode separation of 5 mm. The sample was burned under these conditions for 30 seconds, then increased to $7\frac{1}{2}$ amps for 30 seconds, and finally to 12 amps for 60 seconds. The progressive increase in current helps to completely vaporize all elements present in the sample and consequently register their line spectra.

Fig. 4. Cross-section of cathode.

National Carbon Special Spectrographic Carbons of 3/16″ diameter were used as electrodes. The upper electrodes or anodes were approximately 20 mm. in length. The cathodes were of the same length but they were shaped as illustrated in Fig. 4. This shape minimizes the wandering of the arc and also helps to retain the unvaporized portion of the sample until the last stages of burning.

A new cathode and anode were used for each sample. The carbons were free of all impurity under the conditions of the investigation and showed no contamination on the test plates which were taken of sample electrodes. A special drilling tool was employed to shape the cathodes and precautions were taken to see that no contamination occurred from this source. The composition of the drilling tool included iron, manganese, chromium, and a trace of nickel. However, these elements did not appear at all when sample electrodes were burned in the arc as mentioned above.

Choice of Spectrographic Method

The arc is especially suitable for the examination of non-conducting material such as diamond. The energy produced in the arc is high enough to excite the spectra of most elements in sufficient intensity. The obvious advantage however, of the arc method over other methods of excitation, is that the sample need not be treated according to more or less complicated chemical procedures. This feature alone eliminates the possibility of contaminating the sample with impurities which frequently occur in reagents even of analytical quality.

As a means of determining the minor constituents in a non-conducting solid such as diamond, it was of great advantage to employ the cathode-layer or "Glimmschicht"[8] technique. This is a special application of the carbon arc method. By means of the cathode-layer method, smaller quantities of most elements present in the powdered substance can be detected, than with the spark or other arc methods in spectrum analysis. The great sensitivity of the cathode-layer method is the primary reason for its choice in this investigation. In addition, this method requires only a minute quantity of material for maximum sensitivity. Only 7 mg. of finely powdered substance was used for the analysis of each sample.

An attempt was made to establish the presence or absence of thirty different elements. They are listed in Table 3 along with the most sensitive line and the checking line for each element in the spectral region 2800-4600 Å.

Results of Spectrographic Analysis

It is important to emphasize the fact that this analysis is only semi-quantitative in nature. No effort was made to determine the absolute quantity of the concentration of impurities present in the diamonds. The

[8] Strock, L. W., Spectrum Analysis with the Carbon Arc Cathode Layer ("Glimmschicht"), Adam Hilger, Ltd., London **(1936)**.

analysis is qualitative in nature with a visual estimation of the relative line blackenings. The symbols used to represent the different relative quantities are explained in Table 5, and they are purely arbitrary. The sensitivity varies from element to element, and *L* in the case of one element may represent 0.1%, while in another it may be about .01%, these figures being typical for quartz. Taking into consideration the conditions of excitation, exposure, amount of sample, etc., it may be said that the limits of sensitivity of the minor constituents in diamond are comparable to those of quartz.

TABLE 3

Element Sought	Most Sensitive Line	Check Line	Element Sought	Most Sensitive Line	Check Line
Aluminum Al	3961.53	3944.03	Magnesium Mg	2852.13	3096.92
Antimony Sb	3267.48	3232.52	Manganese Mn	4030.76	4033.07
Arsenic As	2860.46	2898.73	Nickel Ni	3414.77	3524.54
Barium Ba	4554.04		Potassium K	4047.22	4044.16
Beryllium Be	3130.42	3131.06	Rubidium Rb	4215.58	4201.81
Bismuth Bi	3067.73	2897.98	Scandium Sc	4246.85	3613.8
Calcium Ca	4226.73	2899.78	Silicon Si	2881.59	3905.52
Chromium Cr	4254.34	4274.80	Silver Ag	3280.67	3382.89
Cobalt Co	3453.51	3405.12	Sodium Na	3302.94	3302.34
Copper Cu	3247.55	3273.96	Strontium Sr	4607.34	4077.71
Germanium Ge	3039.08	3269.50	Tin Sn	3262.33	3034.12
Gold Au	3122.8		Titanium Ti	3349.41	3371.46
Iron Fe	3719.94	3734.14	Tungsten W	4008.76	4294.62
Lead Pb	4057.83	3683.47	Zinc Zn	3345.51	3302.56
Lithium Li	4602.99	3232.67	Zirconium Zr	3391.98	3438.23

The spectra of the diamonds were registered on two plates. A portion of one of the plates is shown in Fig. 5. This figure represents a region of the spectra which includes Si, Ca, Al, and Fe lines. However, the most sensitive lines for Si, Ca, and Fe happen to occur in other portions of the spectra, as indicated in Table 3. This figure serves to show the way certain elements made their appearance in the spectra, and also gives an idea of the dispersion of the instrument.

All of the data derived from the emission spectra of the 33 specimens are tabulated in Table 4. The elements are arranged with those appearing most frequently to the left, and those appearing least frequently to the right. Thirteen of the thirty elements sought for made their appearance during the analysis.

The four elements Al, Si, Ca, and Mg constitute a persistent group which appears in each of the 33 specimens (with the exception of Nos. 23 and 32, in which Mg was not detected). These elements are abundant

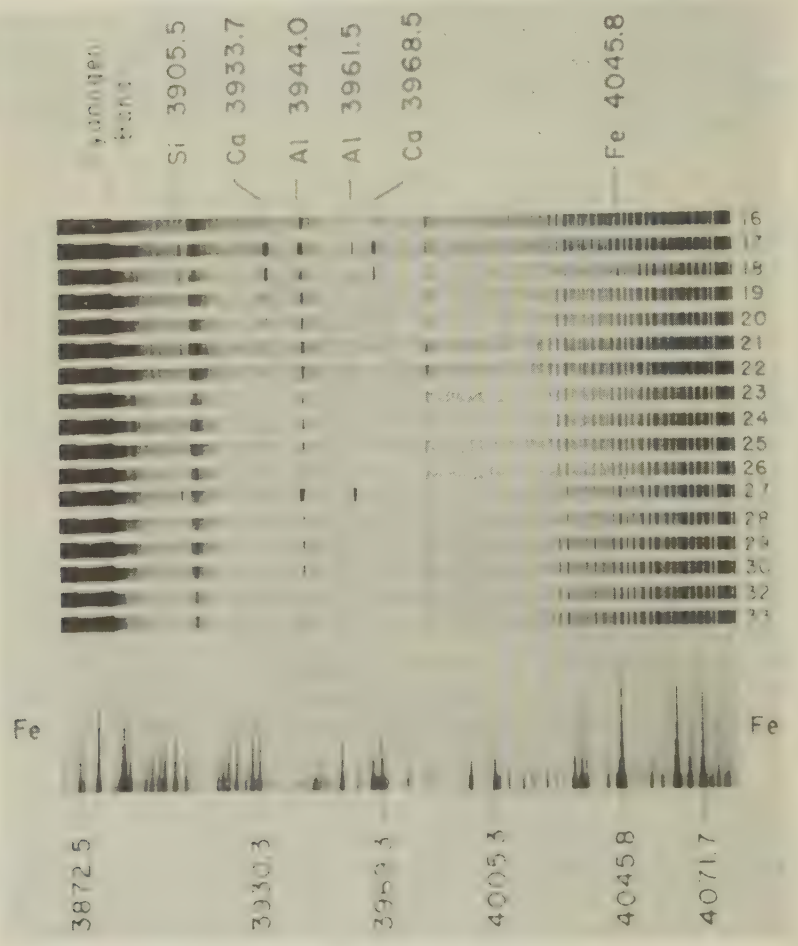

Fig. 5. Portion of spectrographic plate.

in nature and also sensitive to detection by the spectrograph. Al and Si appear to act as a pair of elements which exhibit "sympathetic" variation in each diamond. That is, when Al is large, then Si tends to be large, and when Al is small, Si also tends to be small. The other minor elements,

TABLE 4

Geographic Location See Fig. 1	Diamond No.	Al	Si	Ca	Mg	Cu	Ba	Fe	Sr	Na	Ag	Ti	Cr	Pb	Special Effects
A	1	M	T	M	T	M	L	T	S	T	A	A	S	A	
	2	M	S	M	S	L	M	M	A	T	T	A	A	A	F Z
	3	S	vT	M	T	M−	A	S	S	T	T	T	T	A	
	4	S	T	L	T	S	M	A	A	A	A	A	A	A	F Z
N	5	T	T	S	T	S	M	A	A	A	A	A	A	A	F
	6	S	M	M	S+	S	L	A	M	A	A	A	A	A	F
C	7	M	M	vL	L	S	M+	T	T	A	A	A	A	A	
	8	S	S	M	M	S	M	A	A	A	A	A	A	A	F Z
F	9	S	T	M	S	T	A	T	A	A	T	A	A	A	
	10	S	vT	L	T	T	M+	A	T	A	A	A	A	A	F Z
H	11	M	M+	L	M	S	M+	M	A	T	A	S	A	A	
	12	M+	vL	vL	L	A	L	S	A	S	A	A	A	A	
	13	L	M−	vL	M	T	L	M	L	T	A	S	A	A	
G	14	L	M	S	S	T	A	A	A	A	A	T	A	A	
	15	M	L	M	L	L	A	M	A	T	M	A	vT	S	F
D	16	T	S	S	M	A	A	A	A	A	A	A	A	A	F Z
K	17	vL	L	vL	L	T	vL	M	M	T	A	A	T	A	F Z
	18	vL	L	vL	L	L	vL	M	L	T	T	A	T	A	F
	19	S	S	L	T	T	M	A	A	A	A	A	A	A	F
	20	S+	M	L	S	S	L	A	A	A	A	A	A	A	F
B	21	M	M	M	S	S	L	A	S	A	A	A	A	A	F
	22	M	S	M	T	T	A	A	A	A	A	A	A	A	F
J	23	S	T	S	A	T	M	A	A	A	A	A	A	A	F
	24	M	L	S	M	S	M	S	A	A	T	A	A	A	
L	25	M	M	M	M	S	A	S	T	A	A	A	A	A	
	26	M	M	S	M	T	A	S	A	A	T	S	A	A	
	27	vL	L	M	M	L	M	L	M	A	A	M	S	A	
M	28	M	S+	M	T	T	A	M	A	A	A	A	A	A	F
	29	S	T	S	T	A	A	A	A	A	A	A	A	A	F Z
E	30	S	T	S	T	T	A	A	A	A	T	T	A	A	
	31	M	S	M	S	T	L	M	M	A	T	T	A	A	
I	32	S	T	M	A	T	A	T	A	A	A	A	A	A	
	33	M	M	M	S	T	A	A	A	T	T	A	A	A	

Abbr. vL = very large
L = large
M = medium
S = small
T = trace
vT = very small trace
A = absent
F = fluoresced
Z = zoned

Cu, Ba, Fe, Sr, Na, Ag, Ti, Cr, and Pb show no tendency to persist through all the diamonds, nor is there any sympathetic variation as exhibited by Al and Si.

In some cases an association can be drawn relating the minor element content and geographical location. For example the diamonds from location *K* are divided according to their minor constituents into two pairs, Nos. 17, 18 and 19, 20. Numbers 5 and 6 differ appreciably only in the Sr content. From location *H*, Nos. 11 and 13 are likewise quite similar except for the Sr content. The reason for striking differences between many members from the same geographic region may be that they came from different mines or diggings in that particular locality.

The only correlation which could be observed between color and minor element content concerns the two elements Fe and Ti. Examination of Tables 2 and 4 reveals a tendency for the diamond to be colored when these elements appear individually or simultaneously. However, many other factors affect the color of a substance much more strongly than minor element content. These will not be discussed in the present paper.

A study of the association between minor element content and morphology reveals that diamonds of perfect form, for example Nos. 5 and 6, contain as much minor element content as many of the less perfectly formed diamonds (Nos. 23, 24, etc.). The correlation of habit with impurity content concerns only cubes and octahedra. The octahedra show an absence of Ag and Ti, while the cubes show these two elements to be present. Silver has previously been associated with crystal habit, as shown by Frondel, Newhouse, and Jarrell.[9]

It is unfortunate that approximately 20 elements are not easily detected by the spectrograph. Among those whose presence or absence would be of great interest are B, O, N, P, S, the halogens, etc.

Ultra-Violet Spectroscopy of Diamond

The variations in minor element content as determined by the emission spectra did not suggest a means of distinguishing between the two types of diamond without further information. Robertson, Fox, and Martin[5] have established, among other tests, that the absorption characteristics of the diamond in the ultra-violet region of the spectrum are a criterion for distinguishing between the two types of diamond. The more common or type 1 diamonds exhibit complete absorption at 300 Å, and the rarer or type 2 diamonds absorb at 2250 Å. In so far as one-half of each of the

[9] Frondel, C., Newhouse, W. H., and Jarrell, R. F., The spatial distribution of minor elements in single crystals: *Am. Mineral.*, **26**, 197 (1941).

diamonds was retained, it was possible to use them for ultra-violet absorption measurements.

The purpose of this test was to ascertain whether or not both recognized types of diamond were present in the lot under investigation. If both types were found, then further inspection of the emission data might reveal differentiating characteristics.

The apparatus used for the absorption work consisted of an iron spark as the source of ultra-violet light, and a Hilger Spekker to provide a small concentrated image at the slit of a Hilger Medium Quartz spectrograph. The spectra were recorded on Eastman Process plates. The diamonds were mounted at the slit with a masking arrangement which permitted only light that had passed through the diamond to fall upon the slit. The transmission ability of each diamond so mounted was tested by removing the plate holder and viewing the visible spectrum which was present. Due to the irregular shape and size of some of the diamonds, it was very difficult, and in some cases impossible, to mount the specimen so that adequate light was transmitted for photographing. Even though most of the diamonds possessed an octahedral cleavage, the surface irregularities opposite the cleavage caused them to act as an imperfect lens. Consequently the optic axis of the instrument was disrupted. Diamonds possessing two more or less parallel sides could be mounted and their spectra satisfactorily photographed. Such was the case with Nos. 1, 4, 5, 6, 9, and 29. The absorption spectra of 1, 4, 5, 6, and 9 exhibited a sharp absorption edge at about 3000 Å. The spectra of No. 29 extended to about 2500 Å.

The fact should be kept in mind that this was carried on at ordinary temperatures and that a continuous source of illumination was not used. The test was only qualitative, but nevertheless it qualifies No. 29 as being a type 2 diamond. Nos. 1, 4, 5, 6, and 9 are the common or type 1 diamonds.

Examination of the emission spectra shows that No. 29 is an unusually pure diamond. Traces of two elements and small quantities of two others are all that are indicated, these four elements being members of the persistent group, Al, Si, Ca, and Mg. On this basis it might be predicted that No. 16 is also a type 2 diamond. The surface irregularities of No. 16 prohibited an examination of its absorption spectra.

X-Ray Examination

Single crystal rotation patterns were taken of diamonds Nos. 5, 6, and 9. These specimens were chosen because they possessed quite perfect form and had different impurity content. Numbers 6 and 9 provide a

wide contrast in their content of the heavy elements, Sr and Ba. The patterns were closely examined for spots which would suggest the presence of a superstructure, especially in No. 6. No evidence was found in the specimens examined.

Fluorescence

All of the diamonds in this analysis were examined for fluorescence. It was found that 17 of the 33 diamonds fluoresced under the ultra-violet

Table 5

Diamond No.	Fluorescent Color and Special Effects
2	Light blue inner and outer zone, dark band between
4	Zoned similar to No. 2
5	Yellow
6	Yellow
8	Zoned, yellowish-green outer zone, darker inner zone
10	Octahedron with light colored inner zone
15	Dark blue fluorescence
16	Light inner zone, outer band non-fluorescent
17	Light blue outer region with central dark zone
18	Light blue
19	Yellowish-green
20	Light greenish
21	Brilliant light blue
22	Brilliant light blue
23	Dark yellowish-brown, weakly fluorescent
28	Light blue
29	Light blue band with darker inner zone

light of a mercury vapor lamp. A double 986A red-purple Corex filter, which has a transmission peak at approximately 3650 Å was used. The diamonds which fluoresced are indicated in Table 4, and the fluorescent effects are listed in Table 5. One of the most striking observations made in this test was the evidence for the existence of 'zoning' or zonal growth in seven specimens. These zones were observed as a distinct band of one fluorescent color completely surrounding a central area of quite different fluorescent color. This effect was best noted on the {111} faces which resulted from cleaving the diamonds, as mentioned earlier in the paper. The effect might not have been observed had it not been for the presence of this fresh cleavage surface. The central area in diamonds 2 and 29 was a very distinct triangle. The presence of a triangle on the {111} face would suggest that the early growth of the specimen was octahedral. Its

later growth was also octahedral, but apparently distorted. Upon examination of Tables 4 and 5, there does not seem to be any correlation between the fluorescent effect and the impurity content of the diamonds exhibiting this property. Diamonds which do not fluorescence seem to contain as great a minor element content as diamonds which do exhibit this phenomenon.

Authors of the paper describing the two types of diamond state that flourescent phenomena is common to both types. On the basis of the data from the emission spectra, this might suggest that fluorescence in the diamond could be partially attributed to the members of the persistent group Al, Si, Ca, and Mg.

H. W. Lindley[10] observed in many yellow diamonds from Southwest Africa, a zonal banding parallel to the octahedral faces. He also observed that crystals showing a strong pale blue fluorescence are more transparent than others to ultra-violet light. This observation is confirmed by the findings of this investigation which shows that No. 29 fluoresces pale blue and is quite transparent to ultra-violet light.

Neutron Bombardment

With the possibility in mind that some unusual effect might be induced, the entire collection of diamond fragments (Nos. 1–33 inclusive) was exposed to bombardment by stray, slow neutrons from the M. I. T. Cyclotron for approximately 48 hours. Observations made immediately after removal, and again at three and six days after removal from the cyclotron, revealed no change in appearance of the diamonds. This work was carried out with the collaboration of Dr. Clark Goodman of the Physics Dept. at M. I. T.

Summary

1. The emission spectra in the region 2800–4600 Å of 33 diamonds have been recorded. The data so obtained have been discussed on the basis of geographic location, form, color, *x*-ray pattern, and fluorescence.

2. Analysis was made for thirty elements, and thirteen elements appeared among the thirty-three specimens. They were Al, Si, Ca, Mg, Cu, Fe, Ba, Sr, Na, Ag, Ti, Cr, and Pb. A persistent group of elements, Al, Si, and Ca, was detected in every diamond. The elements Al and Si exhibited 'sympathetic' variation.

3. Absorption spectra in the ultra-violet region have been photographed for six of the diamonds. Five of these were found to be the common or type 1 diamond, and one was the rarer or type 2 diamond (No.

[10] Lindley, H. W., Wachstumserscheinungen am Diamant: *Fortsehr. Min. Krist. Petr.*, **21**, 71 (1937).

29). This diamond proved to be the purest of the lot on the basis of the emission spectra.

4. The diamonds of cubic habit revealed the presence of Ag and Ti, whereas these elements were not detected together in the octahedral diamonds.

5. The elements Fe and Ti tended to be present in the colored diamonds.

6. Similarities were observed in the emission spectra of diamonds from some of the geographical localities.

7. Seventeen of the diamonds exhibited fluorescence. No correlation could be observed between this phenomenon and the minor element content of the specimens. Seven of the fluorescent diamonds showed a zoning effect.

Acknowledgments

The writer is indebted to several persons without whose help this investigation would have been impossible. In the first place the writer wishes to express his gratitude to Amos J. Shaler and J. K. Smit and Sons, Inc., for supplying the diamonds and later cleaving them. Mr. Shaler was also kind enough to assist in preparing the samples for the emission spectrographic analysis. Grateful acknowledgment is made to Prof. M. J. Buerger not only for suggesting this work but for many helpful discussions and for critically reviewing the manuscript. Professor W. H. Newhouse kindly permitted the writer to use the facilities of the Cabot Spectrographic Laboratory. The writer wishes to express his appreciation for advice given by R. F. Jarrell concerning the spectrographic analyses.

ORBICULAR ROCK FROM BUFFALO HUMP, IDAHO[1]

G. E. Goodspeed, *University of Washington, Seattle, Washington.*

Abstract

Within the area of the Idaho batholith, remnants of schist presumably of the Belt series, contain zones of orbicular rocks. The orbicules consist mainly of radiating perthitic-like intergrowths of plagioclase. A complete sequence in the schist from groups of feldspar porphyroblasts indicates a metamorphic rather than a magmatic origin. Gradations from a schist with orbicules to a rock composed chiefly of orbicules indicate that this orbicular rock was formed by metasomatic processes.

Buffalo Hump, with an altitude of nearly 9000 feet, forms one of the prominent monadnocks of north central Idaho, and, according to Shenon

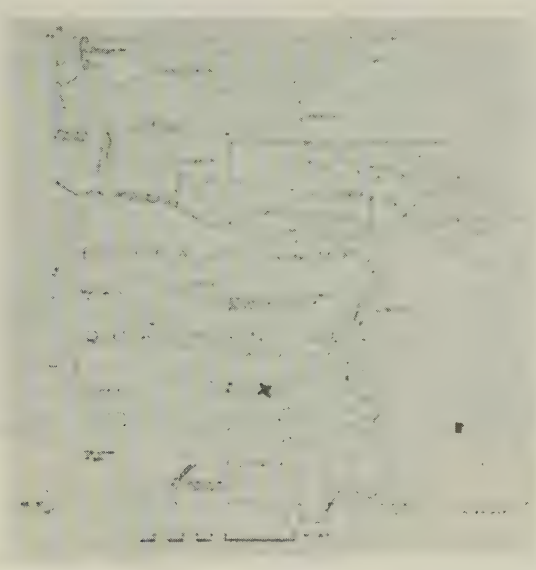

Fig. 1. Index map of Buffalo Hump Quadrangle.

and Reed,[2] rises over a thousand feet above the "so-called" summit of the Idaho peneplain. In their geologic map they show that areas of schist, quartzite, and gneiss, presumably of the Belt series, are nearly equal in extent to the Mesozoic granodioritic rocks of the Idaho batholith. Along a newly constructed mountain road between Calendar and Humptown (Fig. 1), a mile east of Buffalo Hump, several fine outcrops of orbicular

[1] Presented at the annual meeting of the Geological Society of America, Dec. 1940, at Austin, Texas.

[2] Shenon, P. J., and Reed, J. C., Geology and ore deposits of the Elk City, Orogrande, Buffalo Hump and Tenmile districts, Idaho County, Idaho: *Circular* No. 9, *U. S. Geol. Sur.* 1–89 (1934).

rocks are exposed in the road cuts as well as in adjacent glaciated surfaces. These rocks are associated with smaller northerly elongated remnants of schist, and with dike-like masses of pegmatite.

Occurrence of Orbicular Rock

Zones of orbicular rock, approximately 50 feet wide, may be traced parallel to the schistosity for several hundred feet. The orbicules (Fig. 2) in these zones range in size from less than an inch to several inches in diameter. Many of them are fairly regular ovoids with longer axes up to three inches in length. Some of them are more elongated, and a few

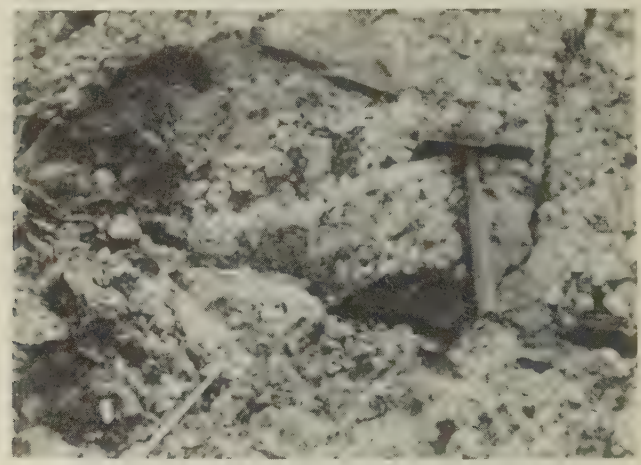

Fig. 2. Orbicular zone and included schist.

are nearly spherical in form. On weathered surfaces the orbicules protrude as egg-shaped masses since they are more resistant to weathering than their enclosing matrix. In road cuts or on fresh glaciated surfaces, white feldspathic orbicules contrast vividly with their darker matrix and exhibit locally irregular or gradational contacts in place of their usual rounded surfaces. Broken orbicules are seen to consist of radiating aggregates of plagioclase with twinning striations readily discernible on some crystals.

Another distinctive feature of some orbicules is the presence of dark cores (Fig. 3) which commonly constitute less than 10 per cent of the orbicules, but which may attain three or four times that figure. A few of these cores consist of tabular fragments of schist which determine the shape of the orbicule. Some of the cores appear to have been recrystal-

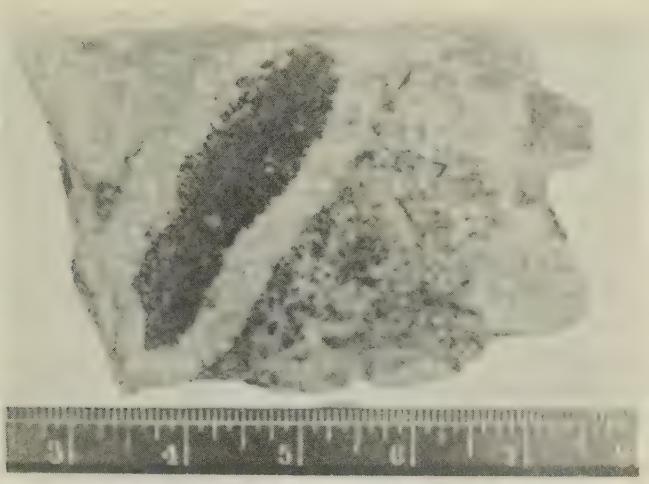

FIG. 3. Orbicule with core of recrystallized schist.

lized showing a concentration of mafic minerals with or without a suggestion of schistosity. Although a few have fairly even contacts with the surrounding aggregates of feldspar, most of them show uneven or grada-

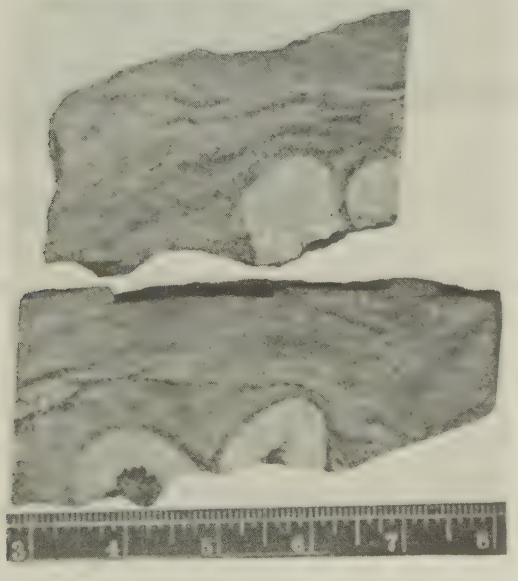

FIG. 4. Polished section of orbicules in schist adjacent to areas of feldspathization.

tional boundaries. A few of the orbicules contain nuclei of biotite which locally is arranged in radial flakes while others exhibit ill defined thin concentric ring-like inclusions of mafics, usually near the periphery.

Although most of the orbicules are closely clustered some are scattered in adjacent fine-grained quartz biotite schist. Some of these feldspar orbicules in forming have apparently pushed aside the schist in a manner similar to a garnet porphyroblast. In polished sections (Fig. 4), a later or secondary schistosity may be seen parallel to the rounded surfaces of these ovoids. The schist immediately adjacent to portions of some of these orbicules shows an increase in mafic minerals as discontinuous concentric zones which locally grade into the feldspar aggregates of the orbicules as well as into the schist. Many of the orbicules surrounded by schist also contain cores of schist or recrystallized schist.

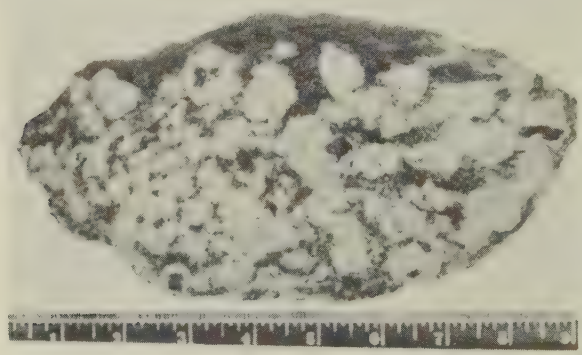

Fig. 5. Feldspar porphyroblasts and incipient orbicules in schist.

In the schist near some of the orbicules there are ill defined feldspar-rich bands roughly parallel to the schistosity and scattered feldspar crystals throughout the schistose matrix. Although some of these crystals are rudely rectangular in outline, many of them are irregular and have gradational contacts with the schist, thus indicating a porphyroblastic origin. Some contain mafic inclusions from the schist in a helixitic-like arrangement. Radial groups of some of these feldspar porphyroblasts (glomeroblastic aggregates) have the appearance of miniature incipient orbicules (Fig. 5). These display transitions from aggregates of porphyroblasts to small but fully formed orbicules, some of which appear to have developed around a core of schist in a concentric shell-like manner, while other groups seem to have coalesced as a unit developing radially from a central point rather than surrounding a fragment of schist.

Where the orbicules are closely clustered they form rounded polygons apparently due to mutual interference, and some actually merge with one another (Fig. 6). Here the matrix loses most of its schistosity, becomes slightly coarser grained in texture and shows a marked increase in crystalloblastic feldspar. Even in some highly orbicular portions, however, relics of thin tabular masses of schist grade into this coarser grained

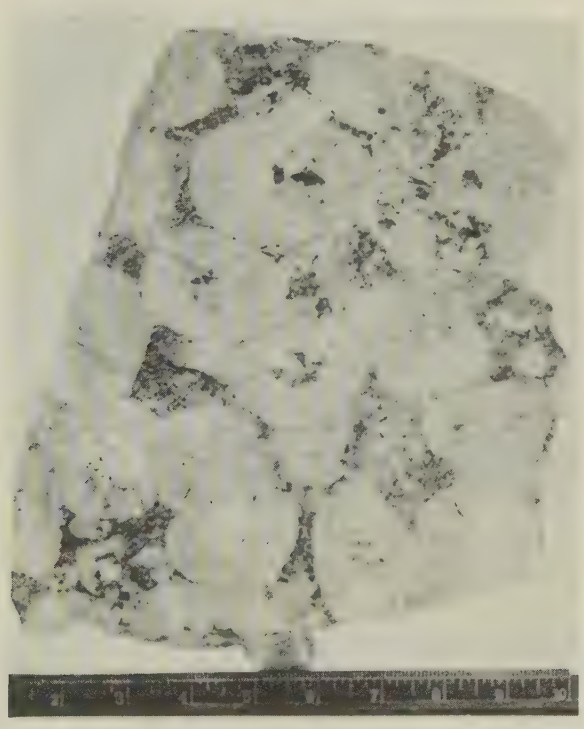

FIG. 6. Closely spaced and merging orbicules.

matrix which otherwise has the appearance of a fine grained granitic rock.

Locally both the matrix and orbicules are transected by small pegmatite dikes and veinlets (Fig. 7). Larger dikes of coarse quartz-feldspar pegmatite are also present in the orbicular zones. The gradational borders of these dikes with the orbicular rock and their content of relics of orbicules indicates that the later pegmatization has obliterated an earlier orbicular structure (Fig. 8). The pegmatized orbicular rock shows numerous slickensided surfaces along which elongated flakes of muscovite or biotite are common. Discontinuous slickensided surfaces are also

FIG. 7. Pegmatitic veinlets transecting orbicules.

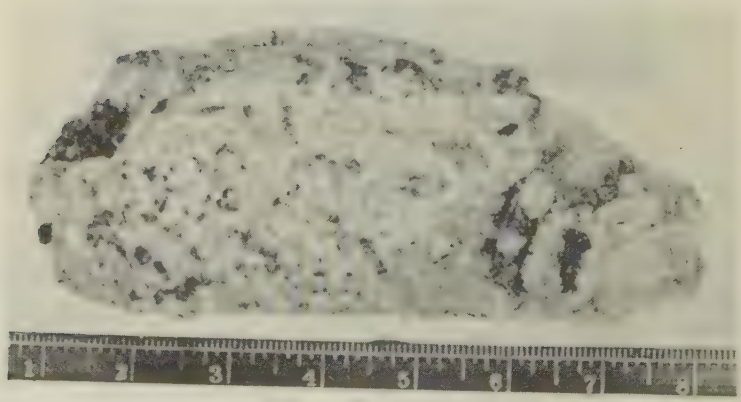

FIG. 8. Gradation of pegmatite into orbicular rock.

present in the orbicular rock. Some of these planes of fracture are bordered with a veneer of pegmatitic material, some transect orbicules, while others appear to have been healed by the development of the orbicules. These slickensided surfaces are commonly irregular and approach somewhat the coarse foliation of contorted metamorphic rocks.

Petrography

The matrix between orbicules shows many variations in texture and mineralogy, ranging from a fine grained quartz biotite schist to a feldspar-rich or mafic-rich granular rock. The schist is a fine grained grayish rock with megascopic biotite, quartz, and feldspar. Polished sections cut at right angles to the schistosity disclose discontinuous quartz and feldspar veinlets parallel to the schistosity. Feldspathization appears along these veinlets and locally extends into the schist 2 mm. to 10 mm. on each side of the veinlet to form gradational contacts speckled with hornblende.

Under the microscope the schist is seen to consist of a fine aggregate of quartz, plagioclase, flakes of brown biotite in alignment with subordinate amounts of sphene, and garnet. Some of the smaller grains of quartz, about 0.1 mm. in diameter, are well rounded, and their shape indicates a detrital origin. The larger quartz grains average about twice this size and form a part of an interlocking mosaic texture. The plagioclase which is about the same size as the larger quartz grains, is calcic oligoclase, (An_{28}), in composition, and shows irregular boundaries indicative of crystalloblastic origin. Flakes of brown biotite interlocking with quartz and feldspar are about 0.6 mm. in length and 0.3 mm. in width. A few of them contain minute inclusions showing pleochroic haloes. Sphene and garnet occur commonly in small (0.1 mm.) rounded anhedra, although there are a few subhedral grains of these minerals.

In thin sections the quartz-feldspar veinlets traversing the schist adjacent to the orbicules show many features characteristic of replacement veinlets; uneven borders, irregular widths, bridge-like septa of schist, sieve structures caused by included minerals and crystalloblastic extension of the vein minerals. These veinlets also contain hornblende, both as relatively large anhedra (1.5 mm. in diameter), and as subhedral crystals. This mineral appears to have in part replaced biotite. The size of biotite is increased and the amount of sphene in these veinlets is also noticeable in greater quantities than in the schist. Adjacent to these quartz feldspar veinlets and to the associated areas of feldspathization, small (1 or 2 mm.) rounded aggregates of feldspar suggest incipient orbicules.

Under the microscope the orbicules present a striking array of radiating intergrowths. A few are simple sheaf-like aggregates of andesine (An_{34}), elongated parallel to the fast vibration direction. Even where the albite twinning is prominent there may be included plagioclase crystals of various orientations and irregular patches of unstriated feldspar (Fig. 9). In some orbicules earlier andesine (An_{36-37}) seems to have been replaced by later oligoclase-andesine (An_{28-30}). Here the oligoclase surrounds, transects and invades the earlier andesine with embayments typical of re-

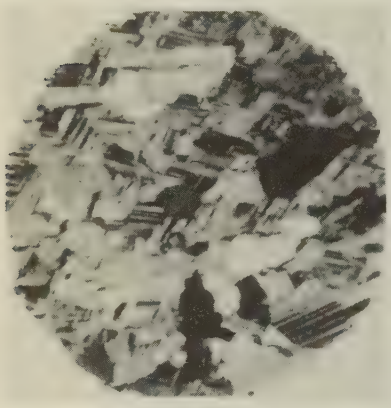

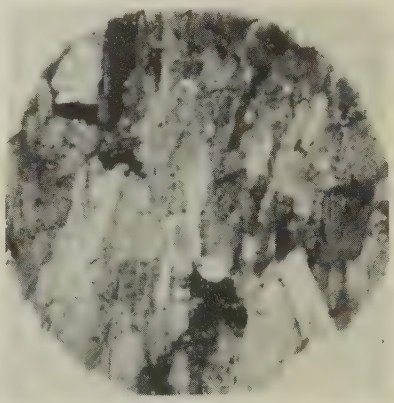

FIG. 9. Photomicrograph from a thin section of an orbicule cut tangentially to the radiating feldspar aggregate.
FIG. 10. Photomicrograph of an orbicule showing a mottled appearance.

placement. Many orbicules show radiating perthitic-like intergrowths which in certain sections produce a crisscross diamond shaped pattern under crossed nicols. The feldspar in other orbicules has a decided mottled appearance (Fig. 10) as though originally it had consisted of many individuals. In some of the feldspars the outline of earlier more calcic included plagioclase is distinct and these crystals may be roughly zoned, the central portion being more calcic. Similar zoning is also present in a few of the larger later feldspars. The plagioclase in some of the orbicules exhibits both albite and pericline twinning, showing the characteristic grid effect. Although resembling microcline these plagioclases have indices of refraction greater than Canada balsam, and they are probably close to andesine (An_{34}) in composition. The twinning lamella of some of the feldspars show a slight amount of curvature usually in areas close to the periphery of an orbicule (Fig. 11). In polished sections some orbicules may be seen to contain minute vugs showing crystal faces of the constituent minerals.

In addition to the inclusion of earlier plagioclase the feldspars of the orbicules contain scattered grains of zoisite, epidote, quartz, hornblende, garnet, sphene, occasional small crystals of pyrite which may be altered to limonite, and a few flakes of muscovite and chlorite. Zoisite occurs in the feldspar aggregate of the orbicules both interstitially and as included grains. The larger aggregates of quartz are later than the feldspar which

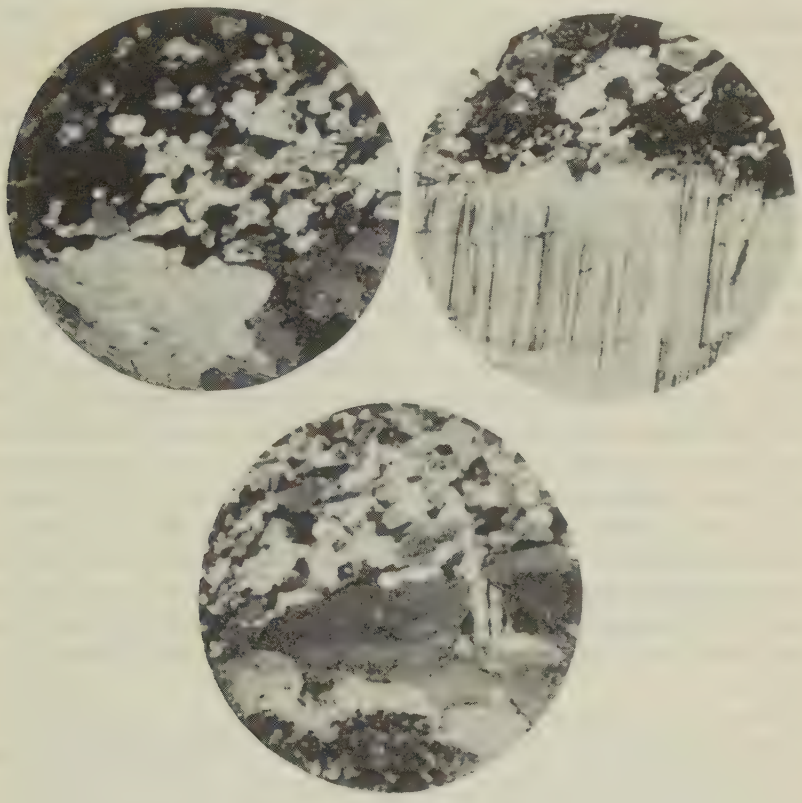

FIG. 11. Photomicrographs showing contact of orbicules and schist.

shows embayments indicative of replacement. A little micropegmatite is present in a few of the orbicules. Most of the feldspars in the orbicules have a turbidity which is due to included kaolinitic material, minute vacuole inclusions, and a very finely divided aggregate which appears to consist of zoisite and sericite. Although this finer included material is as a rule irregular in distribution, it is locally concentrated in certain portions of feldspar aggregates outlining perhaps an earlier feldspar or successive (010) twinning planes.

Some orbicules in schist are surrounded by a secondary schistosity apparently induced by the crystallization of the feldspar, others display locally irregular contacts due both to the inclusion of minerals of the schist in the orbicule and to the extension of the feldspar into the schist. Such crystalloblastic contacts which are most apparent in thin section are accentuated where the matrix is coarser grained and more highly feldspathized. Some sections show an outer zone of clear untwinned more sodic feldspar interlocking with the minerals of the schist, while the more calcic plagioclase toward the central portion of the orbicules, is polysynthetically twinned (Fig. 11). Slight bending of the twinning lamellae may be due to crystallization pressure. The projection of relatively slim extensions of the matrix into the orbicule indicates the absence of mass movement demanded by magmatic flow.

As seen in thin section, the common characteristic of the coarser granular matrix is the crystalloblastic habit of the constituent minerals. Typical sieve structures are common. Hornblende contains numerous rounded grains of quartz similar to the grains in the original schist and forms an irregular interlocking mosaic with quartz and feldspar. Some of the biotite occurs in small flamboyant aggregates and irregular flakes which surround other minerals. Paragenesis may be complex; some of the hornblende appears to be derived in part from an earlier biotite, while some of the biotite is later than the hornblende. In some thin sections of the matrix there is an increase in the amount of hornblende, biotite, sphene, and garnet. Zircon is also noticeable and a few crystals of pyrite are present. Plagioclase is distinctly of a crystalloblastic habit with irregular interlocking boundaries and abundant included grains of quartz and hornblende. Larger plagioclase crystals are typical porphyroblasts. Some later quartz and a little myrmekite, chlorite, and kaolinitic material are present.

Where many orbicules have become fully developed and are closely spaced, the matrix may almost disappear as the orbicules merge with one another. In such orbicules it is common to find a concentric ring of mafics which probably represents an early boundary of the orbicule now enclosed by continued or recurrent feldspathization, which extended the orbicule beyond its earlier limit.

Conclusions

Johannsen gives a complete summary of many types of orbicular rocks, and according to genesis has grouped orbicular granites as: (1) produced by the assimilation of foreign inclusions, (2) produced by portions of more basic or more acid segregations previously separated from the same magma, (3) group of so-called pudding granites, and (4) rocks

whose structures are primary or due to endomorphic contact action.[3] In a recent paper Eskola points out that the interpretation of orbicular rocks as examples of magmatic differentiation has had very far reaching consequences for petrogenic ideas in general.[4] He concludes that esboitic (plagioclase-rich) orbicular rock has been formed by concretionary crystallization due to a metasomatic replacement of pre-existing minerals.

A summary of the significant features of the orbicular rock from Buffalo Hump, Idaho, is as follows: (1) some orbicules occur in schist of probable sedimentary origin; (2) these orbicules in themselves are not schistose; (3) a secondary schistosity in the schist around these orbicules is noticeable; (4) many orbicules have cores of schist or recrystallized schist; (5) replacement intergrowths and relics are common in the orbicules; (6) orbicules characteristically exhibit crystalloblastic contacts with granular matrix and other orbicules; (7) minerals common to metamorphic rocks are associated with the orbicular rocks; (8) minute vug-like cavities are noticeable in some orbicules; (9) orbicules occur adjacent to locii of feldspathization; (10) various stages of development from groups of feldspar porphyroblasts to fully formed orbicules are present.

This evidence, and especially the last two points just listed, indicates to the writer that the orbicules were formed in the schist as a result of metasomatic action of quartz feldspar-rich solutions penetrating local zones of fracture. The concretionary growth of the orbicules would have absorbed the mafic constituents of the schist and would have concentrated these constituents either in the cores of the ovoidal masses or at their peripheries. The secondary schistosity presumably was induced by the growth of the radiating aggregate. The orbicular rock at this locality is, therefore, an example of metamorphic rather than magmatic differentiation.[5]

[3] Johannsen, A., Descriptive Petrography of the Igneous Rocks: *Univ. Chicago Press* (1932).

[4] Eskola, Pentti, On the esboitic crystallization of orbicular rocks: *Jour. Geology*, **46**, (No. 3), 448–486, April–May (1938).

[5] Eskola Pentti, On the principles of metamorphic differentiation; Extrait des *Comptes Rendus de la Societe geologique de Finlande*, N: 05, (**1932**).

NEW DATA ON HETAEROLITE, HYDROHETAEROLITE, CORONADITE, AND HOLLANDITE

CLIFFORD FRONDEL AND E. WM. HEINRICH,
*Harvard University, Cambridge, Massachusetts.**

ABSTRACT

Hetaerolite, $ZnMn_2O_4$, is isostructural with hausmannite, $MnMn_2O_4$. Weissenberg x-ray study of type hetaerolite gave: $a_0=5.74$, $c_0=9.15$; $a_0:c_0=1:1.594$, $a:c=1.5952$ (morph.); cell contents $Zn_4Mn_8O_{16}$. The hetaerolite described by Palache in 1928 from Sterling Hill and Franklin, New Jersey, is identical with the original hetaerolite of Moore (1877) from Sterling Hill.

The so-called hetaerolite from Sterling Hill described by Palache and Schaller in 1910 apparently is the same as that from Leadville, Colorado, described by Ford and Bradley in 1913. The Leadville mineral, for which the name hydrohetaerolite has been proposed, differs from type hetaerolite in its fibrous character, in x-ray cell dimensions ($a_0=5.71$, $c_0=9.04$; body-centered tetragonal (?)), in slightly lower indices of refraction, and in apparently containing a few per cent each of SiO_2 and H_2O. Proof of tetragonal symmetry and of homogeneity is lacking. The status of the mineral is uncertain.

Coronadite is a valid species and is isostructural with hollandite. Hollandite has been thought to be tetragonal from uncertain morphological evidence, but x-ray powder study suggests that it and coronadite are only pseudotetragonal. Coronadite has the composition $MnPbMn_6O_{14}$. The composition of hollandite is uncertain, but the mineral appears to be the barium analogue, $MnBaMn_6O_{14}$, of coronadite. Psilomelane (17% BaO) and hollandite are distinct species.

HETAEROLITE

The name hetaerolite was given by Moore in 1877 to a massive mineral found with chalcophanite at Sterling Hill, New Jersey. Moore stated that the mineral had the composition $ZnMn_2O_4$, analogous to hausmannite, $MnMn_2O_4$, but he did not quote the figures of his analysis nor did he describe the physical and chemical properties in sufficient detail to adequately characterize the substance. In 1910, Palache published an analysis made by Schaller in 1906 of a fibrous mineral from Sterling Hill that was thought to be identical with the original hetaerolite of Moore. The water reported in the analysis (column 2, Table 1) was regarded as due to admixed chalcophanite and the formula $ZnMn_2O_4$, originally suggested by Moore, was assigned to the mineral. A few years later, in 1913, Ford and Bradley described a fibrous mineral found with chalcophanite in the Wolftone mine, Leadville, Colorado. The analysis by Bradley (column 3, Table 1) gave the formula $Zn_2Mn_4O_8 \cdot H_2O$, after the deduction of about 10 per cent hemimorphite which was supposed to be present in order to account for the SiO_2 reported. The name hetaerolite was retained for this mineral by Ford and Bradley on the belief that the original

* Contribution from the Department of Mineralogy and Petrography, Harvard University, No. 249.

TABLE 1. ANALYSES AND CELL CONTENTS OF HETAEROLITE, HYDROHETAEROLITE, CORONADITE, AND HOLLANDITE

	1	2	3	4	5	6	7
Mn_2O_3	64.21	60.44	56.00	54.63			
MnO_2					59.60	60.80	65.63
MnO	1.86				8.02	7.12	5.12
ZnO	32.46	33.43	37.56	37.66		0.11	
PbO					28.68	28.66	
BaO					0.23		17.59
Fe_2O_3	0.24	0.77		0.67	0.60	1.10	10.56
Al_2O_3					0.10	0.68	0.94
SiO_2	0.18	1.71	2.69	2.91	0.26		
H_2O	0.19	3.89	4.36	3.78	1.80	1.11	
Rem.	0.49				0.52	0.42	
Total	99.63	100.24	100.61	99.65	99.81	100.00	99.84
G.	5.18	4.85	4.6		5.505 (5.44)	5.246	4.95

CALCULATED ATOMIC CONTENTS OF UNIT CELL

Mn^4					6.25	6.38	6.23
Mn^3	7.71	7.54	6.99	6.82			
Fe^3	0.38	0.09		0.08			1.24 (+Al)
Si	0.03	0.28	0.44	0.48			
Mn^2	0.25				1.03	0.92	0.59
Zn	3.78	4.05	4.52	4.56			
Pb					1.17	1.17	
Ba							0.95
O	15.70	16.06	15.88	15.86			
H_2O	0.10	2.13	2.39	2.07	0.91	0.56	

1. Hetaerolite. Sterling Hill, New Jersey. Rem. is MgO. Bauer's anal. in Palache (1928).

2. Hydrohetaerolite. Sterling Hill, New Jersey. H_2O+ 1.42, H_2O- 2.47. Schaller's anal. in Palache (1910).

3. Hydrohetaerolite. Wolftone mine, Leadville, Colorado. Average of two analyses. Bradley's anal. in Ford and Bradley (1913).

4. Hydrohetaerolite. Leadville, Colorado. Palmer's anal. in Wells (1937).

5. Coronadite. Bou Tazoult, Morocco. Rem. is CaO 0.05, CuO 0.14, P_2O_5 0.03, As_2O_5 0.04, V_2O_5 0.20, CO_2 0.04. Campredon's anal. in Orcel (1933).

6. Coronadite. Coronado vein, Clifton-Morenci, Arizona. Rem. is MoO_3 0.37, CuO 0.05. Recalculated to 100 after deduction of 7.22 insol. and 0.45 alkalies, CaO, MgO, and loss of wt. Hillebrand's anal. in Lindgren and Hillebrand (1904).

7. Hollandite. Kajlidongri, India. Winch's anal. in Fermor (1909).

hetaerolite of Moore was not anhydrous but contained water. Moore said that his mineral yielded a little water in the closed tube. These writers also considered that the water in Schaller's analysis was essential and not due to admixed chalcophanite. A recent re-analysis (column 4, Table 1) by Palmer of the mineral from Leadville is cited by Wells (1937), and this also shows about 4 per cent of water.

In 1928, Palache described a mineral found as pyramidal crystals in the unoxidized ore at Sterling Hill and Franklin, New Jersey. This material was analyzed by Bauer and proved to be anhydrous $ZnMn_2O_4$. Goniometric measurement proved that the mineral was tetragonal and morphologically related to hausmannite. It was then proposed by Palache to adopt Moore's name hetaerolite for the anhydrous mineral, analogous to hausmannite, here recognized, since this was the sense of the original definition. The actual material of Moore, together with the apparently hydrous mineral analyzed by Schaller was separated under the name hydrohetaerolite as a distinct species. The hydrous mineral from Leadville, described by Ford and Bradley, also is to be classed as hydrohetaerolite.

Part of the original specimen of hetaerolite described by Moore and the original specimens of so-called hetaerolite measured and analyzed by Palache and Bauer were available to the writers for study. *X*-ray powder patterns, taken in Fe radiation, of these specimens proved to be identical. The nomenclature used by Palache is, therefore, entirely proper. A Weissenberg *x*-ray examination was made of a measured crystal of hetaerolite. The data obtained are summarized in Table 2, and com-

Table 2. Comparison of Hetaerolite and Hausmannite

	Cell Contents	Space Group	a_0	c_0	$a_0:c_0$ (*x*-ray)	$a:c$ (morph.)	G. (obs.)	G (calc.)	ω	ϵ	Cleavage
Hetaerolite	$Zn_4Mn_8O_{16}$	*I*4/*amd*	5.74	9.15	1.594	1.5952	5.18	5.23	2.35	2.10	{001} imperfect; also {011} and {112}(?)
Hausmannite	$Mn_4Mn_8O_{16}$	*I*4/*amd*	5.75	9.42	1.638	1.6364	4.84	4.84	2.455 ±0.02	2.15 ±0.02	{001} good, {112} and {011} indistinct

pletely confirm the supposed isostructural relation to hausmannite. The *x*-ray data given for hausmannite are from the powder and rotation study of Aminoff (1936). The specific gravity, given in the original description as 4.85, was re-determined on the microbalance and found to be 5.18. An imperfect cleavage on {001} was observed on macroscopic crystals, and one and possibly two additional cleavages were noted in crushed grains under the microscope. The latter cleavages probably correspond to the {011} and {112}, cleavages of hausmannite. The morphological

TABLE 3. *X*-RAY POWDER DIFFRACTION DATA FOR HYDROHETAEROLITE, HETAEROLITE, CORONADITE, AND HOLLANDITE. Fe RADIATION

Hydrohetaerolite				Hetaerolite			Coronadite		Hollandite	
d	*I*	*hkl*	a_0	*d*	*I*	*hkl*	*d*	*I*	*d*	*I*
3.188	1			4.871	1	101	3.466	6	4.957	2
3.006	7	112	5.700	3.045	7	112	3.104	10	3.459	6
2.855	3	200	5.709	2.855	4	200	2.400	4	3.113	10
2.660	9	103	5.700	2.698	9	103	2.205	4	2.475	1
2.455	10	211	5.703	2.460	10	211	2.155	2	2.409	3
2.250	3	004	5.686	2.300	3	004	2.001	1	2.198	3
2.173	1			2.017	3	220	1.960	1	2.173	2
2.019	3	220	5.710	1.792	3	204	1.919	1	1.988	1
1.771	3			1.752	5	105	1.836	2	1.952	1
1.717	5	105	5.690	1.683	4	312	1.742	1	1.916	1
1.677	4	312	5.712	1.616	3	303	1.691	1	1.842	2
1.612	2	303	5.719	1.560	5	321	1.642	2	1.829	2
1.553	5	321	5.686	1.518	8	224	1.591	1	1.747	1
1.506	8	224	5.711	1.430	4	400	1.542	5	1.694	1
1.430	4	400	5.720	1.350	1	206	1.432	1	1.657	3
1.408	2	314	5.700	1.323	3	305	1.400	1	1.631	3
1.311	2	305	5.712	1.277	2	107	1.374	2	1.583	1
1.294	1	332	5.728	1.263	3	413	1.356	2	1.544	5
1.278	1	420	5.717	1.212	1	404	1.298	1	1.435	1
1.261	4	413	5.724	1.169	5	127	1.237	1	1.419	1
1.210	1	404	5.727	1.151	4	008	1.218	1	1.404	1
1.181	1			1.107	4	415	1.148	1	1.363	2
1.159	3	316	5.723	1.089	3	335	1.116	1	1.351	2
1.151	3	334	5.684	1.053	2	521			1.306	2
1.127	3	008	5.700						1.296	1
1.113	3	424	5.720						1.286	1
1.101	4	415	5.719						1.167	1
1.089	3	512	5.724						1.157	1
1.071	5	503	5.728						1.147	1
1.057	3								1.096	2
1.050	2	521	5.693						1.086	2
									1.078	1
									1.055	1
		$a_0=5.709$								
		$c_0=9.037$								
		$c=0.823$								

ratio $a:c=1:1.1280$, given by Palache, refers to the doubled, face-centered structural cell, and becomes $1:1.5952$ in the body-centered unit here taken.

HYDROHETAEROLITE

A small fragment from the type specimen of the fibrous hydrohetaerolite from Leadville described by Ford and Bradley was available for

study. Unfortunately, the identity of the specimen of hydrohetaerolite from Sterling Hill analyzed by Schaller appears to be lost. Several specimens of botryoidal hydrohetaerolite from Sterling Hill stated by Professor Palache to be representative of this mineral were, however, available for study.

An x-ray powder photograph of the Leadville mineral was indexed with the exception of 5 out of 31 lines in terms of a body-centered tetragonal cell with $a_0 = 5.71$ and $c_0 = 9.04$. Fe radiation was employed. The spacing data are given in Table 3. The pattern is very similar to that of hetaerolite, but relative differences in spacings and in the intensity of some lines are apparent. Further, distinct new lines appear on the hydrohetaerolite pattern. Several of these lines were indexed in terms of the cited cell, but efforts to index the others in terms of any tetragonal cell were unsuccessful. The extra lines may be due to admixture (although the sample appeared homogeneous under the microscope), or to a departure from true tetragonal symmetry. X-ray patterns also were made of specimens of so-called hydrohetaerolite from Sterling Hill. These specimens proved to be gross mixtures of chalcophanite with another mineral which could not definitely be shown to be hetaerolite or hydrohetaerolite because the critical lines were obscured by overlapping chalcophanite lines and by general fogging. The impression was gained, however, that hydrohetaerolite was present.

X-ray rotation and 0-layer and 1-layer Weissenberg photographs were taken about the fiber axis of a minute ($0.1 \times 0.05 \times 0.4$ mm.) fiber of the Leadville mineral. The films were of poor quality due to sub-parallel aggregation and a slight twisting in the fiber. The fiber-period was 8.0 ± 0.1 Å. Both the 0- and 1-layer Weissenberg films had the plane symmetry C_{2i}, with a two-fold axis of symmetry and planes of symmetry at 90°. The poor quality of the films, however, renders their true symmetry content uncertain. The (apparent) symmetry content of the films restricts the symmetry and orientation of the fibers to five possibilities:

(1) Orthorhombic, with the centrosymmetry V_h, and the rotation axis either [100], [010] or [001].

(2) Tetragonal, with the centrosymmetry D_{4h}, and the rotation axis either [100], [010] or [110].

(3) Hexagonal, with the centrosymmetry D_{6h}, and the rotation axis either $[10\bar{1}0]$, $[01\bar{1}0]$ or $[\bar{1}100]$.

(4) Isometric, with the centrosymmetry T_h, and the rotation axis either [100], [010] or [001].

(5) Isometric, with the centrosymmetry O_h, and the rotation axis either [110], [101] or [011].

The isometric possibilities are excluded by optical characters, but the other three possibilities can not be distinguished by the evidence at hand.

The tetragonal interpretation, however, is in accordance with the symmetry and cell dimensions obtained by the powder method. The fiber-period 8.0 ± 0.1Å, is close to the calculated period (8.07 Å) of the [110] direction of the powder cell, and the periods of the simplest cell defined by the 0-layer Weissenberg film, 8.99 and 8.07 Å, correspond to periods ($c_0 = 9.04$, $d_{111} = 8.07$) of the powder cell. Both [110] and [001] would appear on the 0-layer film if the rotation axis was [110]. The systematic omissions on the Weissenberg films lead to the partial space group $I4/a\ d$, if tetragonal symmetry and a [110] orientation are assumed.

Optically, the Leadville mineral appears to be uniaxial negative. Larsen (1921) gives the indices as $\omega = 2.26 \pm 0.02$, $\epsilon = 2.10 \pm 0.02$. Larsen (1921) records the indices of hetaerolite from Franklin as $\omega = 2.34 \pm 0.02$, $\epsilon = 2.14 \pm 0.02$; Berman (cited in Palache (1928)) gives the indices of hetaerolite from Sterling Hill as $\omega = 2.35 \pm 0.02$, $\epsilon = 2.10 \pm 0.02$. Larsen states that the elongation of the fibers is positive, and the writers have found this to be true in most instances, but not for all of the fibers. On the reflecting goniometer almost all of the fibers exhibit up to six or eight cleavage surfaces at what appear (for the most part) to be random angles. The random arrangement doubtlessly is due to an intergrowth. One set of parallel faces occurs on many fibers. Most fibers, if not markedly composite, give a more or less perfect uniaxial optic axis figure. The optical data indicate that the mineral has at least one good cleavage in the elongation, and that the elongation must be perpendicular to [001] of a tetragonal mineral. The fiber used in the Weissenberg x-ray study exhibited one good cleavage along the fiber length. This cleavage was identified by the instrumental correlation between the x-ray and reflecting goniometers as {001} in the (apparent) tetragonal cell, and the direction of elongation, as already noted, appears to be [110]. The optical and x-ray data thus are consistent.

The hydrohetaerolite from Leadville and true hetaerolite are now seen to be very similar. The partial space group $I4/a\ d$ (?) and cleavage of hydrohetaerolite is consistent with the space group ($I4/amd$) and cleavage of hetaerolite. The color, luster, and hardness of the two minerals are practically identical. The specific gravity of hydrohetaerolite is relatively low, but the reported value, 4.65, is questionable because of the fibrous nature of the material. The writers failed to get values above 4.65 on the microbalance. Hydrohetaerolite differs from hetaerolite principally in its somewhat lower indices of refraction, in its smaller cell dimensions, and in the presence of a few per cent each of H_2O and SiO_2.

The atomic contents of the (apparent) tetragonal unit cell are given for the three existing analyses in Table 1. A specific gravity of 5.51 was

assumed for the purposes of the calculation; irrational cell contents are obtained if the observed specific gravities are used. The cell contents of the material from Sterling Hill analyzed by Schaller (column 2) are almost exactly $Zn_4(Mn, Si)_8O_{16} \cdot 2H_2O$, with Si:Mn = 0.148:3.852. The two analyses of the material from Leadville (columns 2, 3) show a small excess of Zn, about equal to the Si, when calculated on this basis. The cell contents of the Leadville mineral possibly may be $Zn_4(Mn, Zn, Si)_8O_{16} \cdot 2H_2O$. If the Si is deducted as hemimorphite, the cell contents are close to $Zn_4Mn_8O_{16} \cdot 2H_2O$ and the simplest formula is $ZnMn_2O_4 \cdot H_2O$, as argued by Ford and Bradley. In any case, it is difficult to accept the high value 5.51 for the specific gravity required for rational cell contents, especially in view of the fact that the calculated specific gravity of anhydrous $ZnMn_2O_4$ is only 5.23. The crystallographic and chemical characters of hydrohetaerolite are uncertain, as is its relation to hetaerolite, and the mineral can at present be classed only as a doubtful species.

Coronadite and Hollandite

Coronadite was originally described by Lindgren and Hillebrand in 1905 from the Coronado vein, Clifton-Morenci district, Arizona. The status of the mineral was brought into doubt by Fairbanks (1923), who examined a specimen in polished section and stated that it was a mixture of hollandite and an unidentified lead mineral. Later, in 1933, Lindgren drew attention to a description by Orcel (1932) of a mineral from Bou Tazoult, Morocco, apparently identical in physical and chemical properties with the original coronadite, and on this ground maintained the validity of the species. At both occurrences the mineral forms dense fibrous masses and crystallographic data are lacking.

A piece of the type-analyzed specimen of the coronadite from Morocco* and the specimen of the coronadite from Arizona, examined by Fairbanks, were available to the writers. The latter specimen is not part of the type material of Lindgren and Hillebrand, but it was examined by Lindgren in 1933 and was accepted as authentic. *X*-ray powder photographs taken in Fe radiation of the two specimens were identical, confirming the opinion of Lindgren as to the identity of the two minerals. The coronadite patterns differed entirely from the patterns of cesarolite, quenselite, manganite, psilomelane (17% BaO) and pyrolusite. The patterns were identical, however, with the pattern of hollandite from Kajlidongri, India. The specimens of hollandite consisted of large, coarse crystals embedded in quartz and were unquestionably authentic. The powder diffraction data for the two minerals are given in Table 2. Fermor,

* This specimen was presented by Orcel to Lindgren and is now preserved in the mineral collection of the Massachusetts Institute of Technology.

in 1909, considered hollandite to be pseudotetragonal and possibly triclinic or orthorhombic. However, in 1917 he measured rough and striated crystals of the mineral and considered them to be tetragonal dipyramidal, with $a:c=1:0.2039$.

Efforts to completely index the powder patterns of coronadite and hollandite in terms of a tetragonal cell were unsuccessful. The patterns, however, were indexed with the exception of a few lines in terms of a body-centered (pseudo-) tetragonal cell with $a_0=6.94$, $c_0=5.71$ for hollandite, and $a_0=6.95$, $c_0=5.72$ for coronadite. The ratio of the cell sides, $a_0:c_0=1:0.823$, is almost four times the axial ratio of Fermor for hollandite. The analyses and atomic contents of the pseudo-cells are itemized in columns 5 and 6 of Table 1. The close approach to a simple ratio of the atomic cell contents of coronadite suggests that the volume of the pseudo-cell bears a simple relation to that of the true cell. The formula of coronadite clearly is $MnPbMn_6O_{14}$ or $MnPbMn_6O_{14}\cdot H_2O$. Water is lacking in the analysis of the isostructural mineral hollandite, and this fact, together with the probable presence of hydrous impurities and capillary water in the analyzed samples of coronadite, make it likely that the mineral actually is anhydrous. The formulae $2MnO_2\cdot PbO$ and $3MnO_2\cdot RO$ were given by Orcel and by Hillebrand, respectively. The value for the specific gravity used in the calculations was 5.44. This value was the highest of eight new determinations on material from Morocco, made on the microbalance, and is preferred to the value 5.505 of Orcel and the value 5.246 of Lindgren and Hillebrand.

The isostructural relation of hollandite and coronadite indicates that the two minerals should have the same general formula. The analysis of hollandite (column 7, Table 1) immediately suggests that the mineral is the barium analogue of coronadite. The calculated atomic ratio of hollandite, however, deviates from the ratio of coronadite in an irrational excess of trivalent metals and a deficiency of divalent manganese. The analysis is stated to have been made in a rough jungle laboratory and its accuracy may be questioned. Possibly some or all of the Fe^3 actually is present as Fe^2 in substitution for Mn^2. If this is the case, the formula may be $(Mn, Fe)BaMn_6O_{14}$. A new analysis on material of demonstrated homogeneity is needed.

Fermor's belief that hollandite is the coarsely crystalline equivalent of psilomelane, and is either identical with or closely allied to romanechite, proves to be without foundation. The powder patterns of hollandite and psilomelane (17% BaO) are entirely unlike, and while both minerals are essentially oxides of Ba, Mn^2 and Mn^4, their atomic ratios appear to be different. An *x*-ray study by Vaux (1937) and unpublished *x*-ray work by one of the writers (C.F.) has shown that romanechite is

identical with psilomelane. According to Vaux, psilomelane is orthorhombic, with $a_0 = 9.1$, $b_0 = 13.7$, $c_0 = 2.86$, and has the general formula $H_4R_2Mn_8O_{20}$, where $R = Mn^2$, Ba, Mg, Ca, Co, Cu, and Ni. In the reported analyses of known psilomelane, Mn^2 and Ba are in the approximate ratio 1:1, with Ba corresponding to *ca.* 17 per cent BaO, and the other divalent constituents are ordinarily present in amounts of one per cent or less of RO.

References

Aminoff, G., *Zeits. Krist.*, **64,** 475 (1936).
Fairbanks, E. E., *Am. Mineral.*, **8,** 209 (1923).
Fermor, L. L., *Mem. Geol. Surv. India*, **37,** 87 (1909).
———, *Rec. Geol. Surv. India*, **48,** [3], 103 (1917).
Ford, W. E., and Bradley, W. M., *Am. Jour. Sci.*, **35,** 600 (1910).
Lindgren, W., and Hillebrand, W. F., *Am. Jour. Sci.*, **18,** 448 (1904).
Lindgren, W., *Am. Mineral.*, **18,** 548 (1933).
Moore, E. S., *Am. Jour. Sci.*, **14,** 423 (1877).
Orcel, J., *C. R.*, **194,** 1956 (1932).
Palache, C., *Am. Jour. Sci.*, **29,** 180 (1910).
———, *Am. Mineral.*, **13,** 297 (1928).
Wells, R. C., *U. S. Geol. Surv., Bull.* **878,** 91 (1937).
Vaux, G., *Mineral. Mag.*, **24,** 521 (1937).

NOTES AND NEWS

INTERFERENCE FIGURES WITH GREATER CONTRAST[1]

WILDER D. FOSTER[2]

The contrast between interference figures and the background can be increased by the use of an iris or fixed diaphragm between the lower nicol prism and the microscope lamp. The efficacy of this diaphragm varies considerably with the type of microscope employed.

A Leitz *SY* microscope was used with a two-iris diaphragm substage and a Spencer microscope lamp with a 110-volt, 100-watt projection bulb. With this model, closing the lower iris diaphragm cuts out much of the scattered light while interference figures are under observation. This lower iris diaphragm was added originally by the manufacturers to have a correctly located aperture diaphragm to work with the low power condenser when the high power condenser lens is swung out.[3]

The apparent contrast of the interference figures of particles revealed by this procedure is estimated to be about the same as that of particles with about 20 per cent more birefringence, examined by the regular methods for observing interference figures.

Thus in samples containing quartz and feldspar in the less than 20-micron size range, many more interference figures are rendered visible by this procedure than by the usual one.

The interference figures of particles having too much undulatory extinction to be revealed by present procedures, can be rendered visible by closing the slides of the Wright sliding stop eyepiece to produce a much smaller opening than usual and closing the lower iris diaphragm.

This method also was tested using a Bausch & Lomb *LD* microscope, which was the only other type of petrographic microscope available. This had no iris diaphragm below the condenser, so a series of fixed diaphragms was used. It was found that the fixed diaphragm needed an opening of at least 3 mm. and that this had to be placed between the microscope lamp and the mirror, and about 5 cm. from the center of mirror. The interference figure was only slightly benefited by such a diaphragm.

It is possible that with some types of microscopes the correct position of the diaphragm might be inside the lower nicol.

[1] Published by permission of the Director, Bureau of Mines, U. S. Department of the Interior.

[2] Assistant Chemist-Petrographer, Gas and Dust Section, Central Experiment Station, Bureau of Mines, Pittsburgh, Pa.

[3] Berek, M., New attachments for the polarizing microscope: *Zeits. Krist.*, **55**, 615 626 (1920).

The author wishes to thank Dr. William J. McCaughey, Ohio State University, and Dr. Herbert Insley, National Bureau of Standards, for their comments and criticisms.

ADDITIONAL NOTES ON THE FINAL GRINDING OF PETROGRAPHIC THIN SECTIONS

A. F. Frederickson, *Montana School of Mines, Butte, Montana.*

Introduction

Not infrequently, while grinding thin sections by hand to the proper thickness, many sections are ground down on one edge while the other edge remains relatively thick. On further grinding in an attempt to equalize the thickness, the thin side, often the portion that is desired for inspection or for photographic purposes, is frequently lost.

Roedder[1] emphasized the importance of an even final grinding plate along with the necessity for inspection, and suggests a method for obtaining a flat plate. Any advantage of using a light under the grinding plate, however, is doubtful for the section must be removed from the plate and washed before it can be properly inspected.

Regardless of the care taken in reducing the section on the fine lap, a section is often produced that is uneven; and the unevenness must be corrected on the final grinding plate if a satisfactory result is desired. The only way to reduce these unevenly ground slides to uniformity is by differential grinding.

The Technique of Differential Grinding

The reduction of the surface of a section to the desired uniform thickness is a separate problem for each condition of non-uniformity. The problem is one of manipulation or technique that can only be acquired by experience. A few possible situations will be considered.

If the section is wedge shaped the procedure that is best adapted to reducing the thick side is as follows:

A strictly clean, level piece of plate glass is placed on a solid table top and wetted. A small amount of grinding compound is placed on the plate with a spatula or spoon and a small portion is spread out over an area of about one square inch. The hands and all other equipment must be perfectly clean for at this stage one coarse grain of grinding compound or grit may ruin the section. The slide is held with the thumb and the second finger with the index finger over the high portion of the section. With a little practice the section can be so held that it can be picked up off the glass plate at any time and still not have the finger tips contact the glass.

[1] Roedder, Edwin, Notes on final grinding of petrographic thin sections: *Am. Mineral.*, **26,** 568–570 (1941).

The holding of the slide, rather than just pressing on it with the fingers, is important if uniformity of grinding is to be attained. It is difficult to apply a uniform pressure with three fingers but it is relatively easy to apply the proper pressure when using only the index finger for pressing. The hand is held at all times in a relaxed attitude and the pressure applied is seldom more than the weight of the finger itself.

With the slide held properly with the index finger over the thick side of the section, the slide is placed on the wetted square inch of grinding compound that has been spread as thinly as possible on the glass plate. The motion of grinding should be forward with the index finger bearing on the thick portion of the slide and thumb and second finger guiding and holding the other end of the slide to the plate without applying pressure. If the grinding were done on the return stroke the thick end would only be rounded off thus making the section more difficult to reduce to a uniform thickness. No rotary motion should be applied for this would produce a section rounded on the sides and high in the middle.

At frequent intervals the slide should be rinsed with water and examined under the microscope to see how the grinding is progressing. If a slight scratch is felt or heard, grinding should be stopped immediately and the glass plate washed to remove all the grinding compound; the section should likewise receive the same treatment and should be examined to discover the cause of the scratch.

A section that is of the proper thickness on the edges but high in the center presents a more difficult problem to reduce to a standard even thickness without losing a portion of the slide. The reduction of the high portion of the section can be accomplished as previously indicated except the index finger is now placed over the center of the high spot—the middle of the slide—and the other two fingers are held near the end of the slide. Again, the absence of a rotary motion is imperative.

If a section is uniformly ground but thick a rotary motion with the index finger held lightly on the center of the slide produces good results.

Often, in spite of ordinary care, a piece of the section may break loose or a piece of grit may get under the slide and the section scratched or loosened from the balsam. Careful and frequent inspection of the washed section immediately will show a series of colored rings or arcs. Grinding should be stopped if these arcs are observed and the section warmed, but not heated. The portion of the slide that is loose can be recemented into place by pressure applied with the flat head of a nail.

When the section is very thin on one side and thick on the other, additional grinding according to the procedure mentioned above will sometimes remove the thin portion of the section in spite of care. A thin film of balsam spread on the thin end of the slide will permit the reduction of

the high end of the "wedge" and preserve the thin end. Too much balsam, however, should be avoided for a double wedge may be developed.

Conclusion

The author has ground many sections of different types of rocks and has produced hundreds of sections from cataclastic quartz, using the technique here described with very satisfactory results. A few timely remarks about the actual technique of the reduction of uneven sections to a standard thickness has been very useful in guiding those new in the art of grinding sections and, needless to say, has saved many good sections that otherwise might have been lost.

PROCEEDINGS OF SOCIETIES

PHILADELPHIA MINERALOGICAL SOCIETY

Academy of Natural Sciences of Philadelphia, September 4, 1941

Dr. Thomas presided with 52 members and visitors present. The program consisted of receiving reports on summer trips. Mr. Trudell described an excursion to Maryland and Virginia with Messrs. Toothaker, Baldwin and Gordon, and exhibited barite from Frostburg; pyrolusite from Crimora; rhodonite from near Louisa; pyrite, staurolite, tremolite, and gahnite from Mineral; and the usual minerals from Amelia. Mrs. Thomas described a trip to Grafton, N. H. (autunite, gummite and torbernite); North Groton (garnet), and Quebec. Mr. Gordon exhibited axinite from the Perkiomenville, Pa., quarry, a new locality for the mineral. Mr. Evans reported on a trip to Hiddenite and Spruce Pine, and Franklin, N. C. Dr. Lee exhibited aragonite and vivianite from Mullica Hill, N. J., and natrolite from Perkiomenville. Mr. Frankenfield found quartz crystals at Middleville, N. Y., nephelite and sodalite at Bancroft in Ontario, and apatite and sphene at Lake Clear.

October 2, 1941

Dr. Thomas presided with 74 members and visitors present. The following officers were elected for 1941–1942: President: Dr. W. Hersey Thomas; Vice-president: Charles R. Toothaker; Secretary: Forrest L. Lenker; Treasurer: Harry W. Trudell; Councillor: Harold Arndt. Mr. John Vanartsdalen was elected an honorary member. Mr. Charles R. Toothaker addressed the society on "Tubular calcite from Guanajuato." Mr. Gordon gave a Kodochrome illustrated talk on "Collecting Minerals in the Trans-Pecos of Texas."

FORREST L. LENKER, *Secretary*

BOOK REVIEW

NEVADA'S COMMON MINERALS by VINCENT P. GIANNELLA. University of Nevada Bulletin. Geology and Mining Series, No. 36. 110 pages. 1941. Price 50 cents.

This bulletin is a revision and expansion of a previous work by Grawe (University of Nevada Bull., vol. 22, No. 1, 1928). It is designed primarily for the prospector and layman interested in the minerals of Nevada. Part 1 deals with the origin, occurrence, and association of minerals; Part 2 treats of the general characteristics of minerals; and Part 3 records the description of 125 minerals commonly found in the State with tables for their determination based on physical properties. The concluding chapter (Part 4) lists (without description) 400 mineral species that up to the present have been found in Nevada.

W. F. H.

NEW MINERAL NAMES

Selenocosalite

OLOF H. ÖDMAN: Geology and ores of the Boliden deposit, Sweden. *Sveriges Geol. Undersökning, Årsbok* **35** (no. 1), 190 pp. (1941); pp. 87–88.

COMPOSITION: Probably a selenian cosalite, $Pb_2Bi_2(S, Se)_5$, but possibly a selenian galenobismutite, $PbBi_2(S,Se)_4$.

Analyses 1 and 2 below were made on material containing very little chalcopyrite, pyrrhotite, and sternbergite (?), but which was intergrown with galena in fairly large amounts. If chalcopyrite, pyrrhotite, and Ag_2S are deducted, analysis 2 gives molecular ratios:

	Pb	(*Bi*+*Sb*)	(*S*+*Se*+*Te*)	
Analysis 2	214	175	463	
Cosalite	175	175	438,	leaving Pb 39, S 25
Galenobismutite	87	175	350,	" Pb 127, S 113

The statement is made, "Neither of the two calculations can be said to be conclusive and the determination of the mineral as a subspecies of cosalite must be subject to strong reservation."

PHYSICAL AND OPTICAL PROPERTIES: Tin-white and indistinctly lamellar in hand specimen. G. = 7.00. Optically very similar to galena in color and reflectivity. Slightly softer than galena. Pleochroism weak in air, distinct in oil immersion, varying from creamy white to gray with a greenish tint. The anisotropism is distinct. The extinction is somewhat oblique.

OCCURRENCE: Occurs in quartz apophyses and in quartz-tourmaline veins from the 210 m. and 410 m. levels of the Boliden mine, Västerbotten province, northern Sweden.

Selenokobellite

OLOF H. ÖDMAN: *op. cit.*, pp. 89–90.

COMPOSITION—A selenian kobellite, $Pb_2(Bi,Sb)_2(S,Se)_5$?

Analyses 3–6 below were made on homogeneous material containing only small amounts of arsenopyrite, cobaltite, chalcopyrite, sphalerite, bournonite, and an undetermined bismuth telluride, with traces of galena. After deducting these accessory minerals, the following molecular proportions were obtained.

No.	Pb	Bi+Sb	S+Se
3	2	2.1	5.2
4	2	2.3	5.4
5	2	2.4	5.54
6	2	2.7	6.36

The variations are believed to be due to solid solution, rather than to impurities.

PHYSICAL AND OPTICAL PROPERTIES: Whitish gray in hand specimens, somewhat darker than selenocosalite. Somewhat softer than galena. The optical properties are very similar to those of selenocosalite, but the pleochroism is stronger. Anisotropism fairly strong. G. = 6.048–6.573.

OCCURRENCE: Found in quartz-tourmaline veins on the 170 m. and 250 m. levels of the Boliden mine. Sometimes forms separate veins 5–10 cm. thick.

Analyses (by Thelma Berggren)

	1	2	3	4	5	6
Pb	43.51	44.20	39.80	39.98	38.29	36.48
Bi	31.11	31.40	18.91	21.27	21.27	24.35
Sb	2.72	2.88	13.83	15.02	14.75	14.61
S	12.26	12.36	15.95	15.93	15.86	16.89
Se	6.32	6.38	5.66	5.00	5.74	4.78
Te	0.80	0.80	0.21	0.44	0.17	nil.
As	nil.	nil.	0.68	0.10	0.79	0.25
Cu	0.12	0.14	1.57	1.28	1.37	1.50
Fe	0.29	0.29	1.84	0.58	1.02	0.63
Ag	1.18	1.02	0.44	0.39	0.38	0.36
Insol.	1.62	0.66	1.00	nil.	—	nil.
	99.93[a]	100.13[a]	100.15[b]	100.08[c]	100.00[d]	99.85[e]
G.=	7.00	—	6.048	6.481	6.463	6.573

[a] Ni,Co,Zn,Au,nil; [b] also Zn 0.22, Co 0.04, Ni,Au tr.; [c] also Zn 0.09, Ni,Co,nil.; Au tr., Hg, Sn, spectroscopic tr.; [d] also Zn 0.22, Co 0.14, Ni,Au,tr.; recalculated after deducting 0.64% insol.; [e] Ni, Co, Zn, Au, nil. 1–2. Selenocosalite, stope 13, 210 m. level; 3. & 5. Selenokobellite, stope 12, 210 m. level; 4. & 6. Selenokobellite, main east drift, Sec. 11, 210 m. level.

DISCUSSION: Further work, particularly *x*-ray study, is needed for both minerals.

MICHAEL FLEISCHER

Ishkulite

G. P. BARSANOV: Ishkulite—a new mineral of the spinel group. *Comptes Rendus* (Doklady) *Acad. Sci. URSS.* **31,** 468–471 (1941).

NAME: For locality, Ishkul lake.

CHEMICAL PROPERTIES: A magnetite containing some chromium.

Analysis: TiO_2 1.24, Fe_2O_3 61.04, Al_2O_3 0.03, Cr_2O_3 11.19, FeO 24.05, MnO 0.54, MgO 1.31, NiO 0.18, H_2O 0.02, V_2O_5 0.32; sum 99.92. After deducting 2.24% ilmenite and 16.47% Fe_2O_3 (martite), calculation gives $FeFe_2O_4$:$FeCr_2O_4$:$MgFe_2O_4$=8.7:2.5:1. The mineral is infusible. It dissolves with difficulty in conc. HCl on prolonged boiling, and is etched only by boiling conc. HCl or by cold HF.

PHYSICAL PROPERTIES: Color, tarry-black; streak, black. H.=6–6½, G.=5.079. Highly magnetic. Opaque. Isotropic in reflected light.

OCCURRENCE: Found in contact rocks near Ishkul Lake, associated with diopside, actinolite, phlogopite, and calcite.

DISCUSSION: An unnecessary name for chromian magnetite.

M. F.

DISCREDITED SPECIES

Tanatarite

J. D. GOTMAN: On the identity of tanatarite and diaspore. *Compt. Rendus Acad. Sci. URSS,* **31,** 29–30 (1941). Re-examination of type tanatarite (supposed to be monoclinic AlOOH) shows that the optics indicate orthorhombic symmetry. *X*-ray powder pictures of tanatarite and diaspore were identical.

M. F.